

Summer 7-2021

## Modeling of a Hybrid-Electric System and Design of Control Laws for Hybrid-Electric Urban Air Mobility Power Plants

Sohail Bin Salam Lahaji  
sohailbf@my.erau.edu

Follow this and additional works at: <https://commons.erau.edu/edt>



Part of the [Aeronautical Vehicles Commons](#), [Navigation, Guidance, Control and Dynamics Commons](#), and the [Propulsion and Power Commons](#)

---

### Scholarly Commons Citation

Lahaji, Sohail Bin Salam, "Modeling of a Hybrid-Electric System and Design of Control Laws for Hybrid-Electric Urban Air Mobility Power Plants" (2021). *PhD Dissertations and Master's Theses*. 602.  
<https://commons.erau.edu/edt/602>

This Thesis - Open Access is brought to you for free and open access by Scholarly Commons. It has been accepted for inclusion in PhD Dissertations and Master's Theses by an authorized administrator of Scholarly Commons. For more information, please contact [commons@erau.edu](mailto:commons@erau.edu).

MODELING OF A HYBRID-ELECTRIC SYSTEM AND DESIGN OF CONTROL  
LAWS FOR HYBRID-ELECTRIC URBAN AIR MOBILITY POWER PLANTS

By

Sohail Bin Salam Lahaji

A Thesis Submitted to the Faculty of Embry-Riddle Aeronautical University  
In Partial Fulfillment of the Requirements for the Degree of  
Master of Science in Aerospace Engineering

July 2021

Embry-Riddle Aeronautical University

Daytona Beach, Florida

MODELING OF A HYBRID-ELECTRIC SYSTEM AND DESIGN OF CONTROL  
LAWS FOR HYBRID-ELECTRIC URBAN AIR MOBILITY POWER PLANTS

By

Sohail Bin Salam Lahaji

This Thesis was prepared under the direction of the candidate's Thesis Committee Chair, Dr. Richard "Pat" Anderson, Department of Aerospace Engineering, and has been approved by the members of the Thesis Committee. It was submitted to the Office of the Senior Vice President for Academic Affairs and Provost, and was accepted in the partial fulfillment of the requirements for the Degree of Master of Science in Aerospace Engineering.

THESIS COMMITTEE

Chairman, Dr. Richard "Pat" Anderson	Member, Dr. Richard Prazenica
Member, Dr. Patrick Currier	Member, Dr. Kyle Collins
Graduate Program Coordinator, Dr. Daewon Kim	8/4/2021 Date
Dean of the College of Engineering, Dr. Maj Mirmirani	8/4/2021 Date
Associate Provost of Academic Support, Dr. Christopher Grant	8/5/2021 Date

## ACKNOWLEDGEMENTS

First and foremost, I would like to thank almighty Allah for giving me strength to pursue master's in aerospace engineering and complete this thesis.

This thesis work would not have been possible without the help and support of the faculty, student, and staff of the Eagle Flight Research Center (EFRC). I would like to thank Dr. Richard 'Pat' Anderson who is my thesis advisor for his constant guidance, support, and motivation since the beginning of my master's journey at Embry-Riddle Aeronautical University (ERAU). I would also like to thank him for giving me opportunity to work at as graduate research assistant for project Phoenix and other projects at EFRC which helped me pursue my master's degree at ERAU. A special thanks to Dr. Richard Prazenica who not only helped me in my academic course work, but also provided mental and emotional support during my research.

I would like to express my gratitude to Dr. Patrick Currier who offered great technical insight which helped me achieve my goals. Dr. Kyle Collins availability and guidance to assist me throughout my thesis work was invaluable. I am also thankful to Dr. Marc Compere and Dr. Jianhua Liu for their technical expertise and support beyond their duty.

Finally, it is impossible to express my gratitude to my family: Mrs. Parveen Begum (mom), Mr. Salam Bin Jaffer Lahaji (dad), Mrs. Juveria Bin Salam Lahaji (sister) and Mr. Numan Bin Salam Lahaji (brother) for believing and supporting me through the good and the difficult periods of my master's education.

## ABSTRACT

Advanced Air Mobility (AAM) is an emerging market and technology in the aerospace industry. These systems are being developed to overcome traffic congestion. The current designs make use of Distributed Electric Propulsion (DEP): either fully electric or hybrid electric. The hybrid engine system consists of two power sources: prime movers, such as turbine engines, and batteries. The hybrid systems offer higher range and endurance compared with the existing fully electric systems.

Hybrid-electric power generation systems for AAM have different mission requirements when compared to systems used in automobiles. Therefore, there is a particular need to model hybrid-electric systems and the development of control logic specifically for AAM aircraft. This thesis focusses on the modeling and design of control logic for hybrid-electric power plants for Advanced Air Mobility (AAM) applications. The developed model can assist in designing and optimizing the system as well as supporting the system architecture. These models can also help the testing and integration of hardware and software of systems and sub-systems, also known as software-in-the-loop and hardware-in-the-loop simulations.

A state-space representation of the hybrid-electric system is created and validated with experimental results to facilitate the use of modern controls methods. A control law for the hybrid-electric system was also developed to meet the AAM aircraft mission requirement of generating the required electrical power and maintaining the State of Charge (SOC) of the batteries.

## TABLE OF CONTENTS

ACKNOWLEDGEMENTS.....	iii
ABSTRACT.....	iv
LIST OF FIGURES.....	viii
LIST OF TABLES.....	xi
NOMENCLATURE.....	xii
ABBREVIATIONS.....	xiii
1. Introduction.....	1
1.1. Advance Air Mobility.....	1
1.2. Urban Air Mobility.....	3
1.3. Distributed Electrical Propulsion.....	3
1.4. Why Choose Hybrid Electric System for Urban Air Mobility Aircraft? .....	5
1.5. Modelling of Hybrid Electric System.....	7
1.6. Design of Control law for Hybrid Electric System.....	8
1.7. Thesis Objectives.....	9
2. Background and Literature Review.....	12
2.1. Hybrid Electric Propulsion.....	12
2.2. EFRC's Hybrid-Electric System for UAM Applications.....	13
2.2.1. Engine.....	15
2.2.2. Generator.....	16
2.2.3. Battery.....	17
2.2.4. Vehicle Control Unit.....	17
2.3. Battery Single Cell Equivalent Circuit Model.....	18
2.3.1. Idealized Electrical Components.....	18
2.3.2. Equivalent Circuit Model.....	19
2.4. Coulomb Counting Method.....	20
2.5. State-space Representation.....	21
2.5.1. Stability of System.....	23
2.5.2. Controllability.....	23
2.5.3. Observability.....	24
2.6. Full State Feedback Control.....	25
2.7. Control Philosophy of Automotive Hybrid-Electric System.....	26
2.7.1. Rule Based Power Management Control Algorithms.....	27
2.7.2. Offline Power Management Control Algorithms.....	28
2.7.3. Online Power Management Control Algorithms.....	29
2.8. EFRC's Hybrid-Electric Load Following Controller for UAM.....	30
2.8.1. Feedforward Control.....	31
2.8.2. Feedback Control.....	32

2.8.3. SOC Management.....	33
3. Methodology.....	35
3.1. Modeling of Hybrid-Electric System using Idealized Electrical Components.....	35
3.1.1. Internal Combustion Engine.....	35
3.1.2. Generator/Inverter.....	37
3.1.3. Battery Pack.....	39
3.1.4. Aircraft Load / Power Sink.....	41
3.1.5. Free-body Diagram of Hybrid-Electric System.....	42
3.2. Modelling of the System using State-Space Representation.....	43
3.2.1. Derivation of State Differential Equations.....	44
3.2.2. Derivation of Variable Parameter and Other System Parameters.....	45
3.2.3. State-Space Representation of Hybrid-Electric System.....	46
3.2.4. Analysis of State-Space Model of Hybrid-Electric System.....	48
3.3. Controls Requirement of Hybrid-Electric System for UAM Applications.....	49
3.3.1. Mission Power Requirement.....	50
3.3.2. SOC Management Requirement.....	51
3.4. Development of Linear Quadratic Regulator.....	52
3.4.1. Augmented State-Space Representation using Integral State.....	53
3.4.2. Estimating Reference/Desired States.....	54
3.4.3. Tuning LQR Controller.....	55
3.5. Simulation of Hybrid-Electric System.....	56
3.5.1. Open-loop Simulation using Idealized Electrical Elements.....	57
3.5.2. Validation of Idealized Electrical Elements Model.....	60
3.5.3. Open-loop Simulation using State-Space Representation.....	60
3.5.4. Validation of State-Space Model.....	61
3.5.5. Closed-loop Simulation with Modern Linear Quadratic Regulator.....	62
4. Results.....	65
4.1. Results of Open-Loop Idealized Electrical Element Mode.....	65
4.1.1. Generator Current Validation.....	66
4.1.2. Battery Current Validation.....	67
4.1.3. Hybrid-Electric Bus Voltage Validation.....	68
4.1.4. Electric Load Current Validation.....	69
4.2. Results of Open-Loop State-Space Model.....	70
4.2.1. Generator Current Validation.....	70
4.2.2. Hybrid-Electric Bus Voltage Validation.....	71
4.2.3. Hybrid-Electric Battery Current Validation.....	72
4.2.4. Electric Load Current Validation.....	73
4.3. Results of Closed-Loop Model with Modern Linear Quadratic Controller.....	74
4.3.1. Performance of the Controller under Constant Load.....	74
4.3.2. System States and Other Critical Parameters under Constant Load.....	76
4.3.3. Phase-Plane Trajectories under Constant Load.....	77
4.3.4. Performance of the Controller Under typical UAM Power Profile.....	78
4.3.5. System States and Other Parameters under UAM Power Profile.....	79

5. Discussion, Conclusions, and Recommendations.....	80
5.1. Modelling of Hybrid-Electric System.....	80
5.2. Linear Quadratic Controller for Hybrid-Electric System.....	81
5.3. Bus Voltage as Control Parameter.....	82
REFERENCES.....	83



## LIST OF FIGURES

Figure	Page
1.1 NASA: Urban Air Mobility Concept.....	2
1.2 Joby Aviation’s Tilt Rotor Aircraft.....	3
1.3 Verdego Aero: Distributed Electrical Propulsion System.....	4
1.4 Hybrid Electric System for UAM Aircrafts.....	6
1.5 Benefits of Modeling.....	7
1.6 Thesis Development Overview.....	10
2.7 Schematic Diagram of Serial Hybrid Electric System.....	13
2.8 EFRC's Serial Hybrid Electric Power Plant Prototype.....	14
2.9 Schematic Diagram of Hybrid Electric System.....	15
2.10 Rotax 915 iS Engine.....	16
2.11 YASA Generator.....	16
2.12 Samsung 20s Battery Cell.....	17
2.13 dSPACE Controller.....	18
2.14 Idealized Electrical Elements.....	19
2.15 Thevenin Model for Lithium-Ion Battery Cell.....	20
2.16 Pictorial Representation of State Space Form.....	22
2.17 Full State Feedback Control.....	26
2.18 EFRC’s Feedforward and Feedback Control.....	31
2.19 Data to determine the desired throttle position for torque and speed.....	32
2.20 SOC management control logic.....	33

Figure	Page
2.21 SOC Management: Target Current Lookup Table.....	33
3.22 Rotax Torque-Speed- Throttle Map.....	36
3.23 Rotax Engine Torque Vs Throttle Map at 5500 RPM.....	36
3.24 YASA Generator and Cascadia Combined Efficiency Map.....	38
3.25 Generator/ Inverter Variable Current Source with Some internal Resistance.....	39
3.26 Modelling of battery as variable voltage source.....	40
3.27 Experimental results of discharge test of Samsung 20s battery cell.....	41
3.28 Modelling of Aircraft load as variable resistor.....	42
3.29 Free Body Diagram of Hybrid Electric System.....	43
3.30 Control Requirement of Hybrid Electric System.....	49
3.31 Power Requirement of Typical UAM aircraft.....	50
3.32 LQR Controller.....	53
3.33 LQR controller for Augmented System.....	54
3.34 Simulation Workflow.....	57
3.35 Idealized Electrical Element Model.....	58
3.36 SOC Calculator.....	59
3.37 Battery Open Circuit Calculator.....	59
3.38 Validation of Idealized Electrical Element Model.....	60
3.39 State-Space Model of Hybrid Electric System.....	61
3.40 Validation of State-Space Model.....	62
3.41 Closed Loop Simulation with LQR Controller.....	63

Figure	Page
3.42 LQR Controller for Hybrid Electric System.....	64
4.43 Overview of Result from Different Simulation Models.....	65
4.44 Idealized Electrical Element Model: Generator Current Validation.....	66
4.45 Idealized Electrical Element Model; Battery Current Validation.....	67
4.46 Idealized Electrical Element Model: Bus Voltage Validation.....	68
4.47 Idealized Electrical Element Model: Load Current Validation.....	69
4.48 State Space Model: Generator Current validation.....	70
4.49 State Space Model: Bus Voltage Validation.....	71
4.50 State Space Model: Battery Current Validation.....	72
4.51 State-Space Model Validation: Load Current.....	73
4.52 Closed Loop System performance under Constant load.....	75
4.53 System States and other Critical Parameters under Constant Load.....	76
4.54 Phase-Plane Trajectories of the System.....	77
4.55 Performance of the Controller under typical UAM power profile.....	78
4.56 System States and other parameters under typical UAM power profile.....	79

**LIST OF TABLES**

Table	Page
2.1 EFRC's Hybrid-Electric System Components.....	14
2.2 Eigenvalues: Stability of a Linear System.....	24
3.3 Hybrid Electric Components Represented as Idealized Electrical Elements.....	42
3.4 Governing Equations of Hybrid Electric System.....	47

## NOMENCLATURE

$T_{ss}$	Torque at Steady State
$u_1$	Throttle/ Percentage of Power
$T_t, T$	Torque at time (t)
$\tau$	Time Constant
$\alpha_1$	Throttle Constant = $\frac{T_{ss}}{u_1}$
$i_g$	Generator Current
$\alpha_2$	Generator Constant = $\frac{i_g}{T_{ss}}$
$i_b$	Battery Current
$i_l$	Load Current
$V_b$	Battery Terminal Voltage
$V_{oc}$	Battery Open Circuit Voltage
$a1$	SOC Constant
$a2$	Battery Current Constant
$a0$	Battery Constant
$Q_n$	Battery Capacity
$R_l(t)$	Electrical Resistance of Load
$L$	Electrical Load
$\omega$	Shaft Speed in radians per second
$R_g$	Electrical Resistance of Generator
$\eta$	Combined efficiency of Generator and Inverter

**ABBREVIATIONS**

AAM	Advance Air Mobility
DOC	Depth of Charge
DEP	Distributed Electrical Propulsion
ECM	Equivalent Circuit Model
EFRC	Eagle Flight Research Center
SOC	State of Charge
UAM	Urban Air Mobility

## **1. Introduction**

The density of our population is increasing, and urban cities are growing. As a result, transportation through traffic congestion remains a challenge. The solution to these trends can be found in the technological advancement of electric aircraft. Electric aircraft can transform the way goods and people move in and around the traffic of congested urban areas. The basic definition of these technological advancements along with the objective of this thesis are introduced in this chapter.

### **1.1. Advanced Air Mobility (AAM)**

Advanced Air Mobility refers to air transportation that utilizes advanced air vehicles to transport passengers and/or cargo (FAA, 2020). AAM includes most of the cases of aerial operations not specific to urban environments.

### **1.2. Urban Air Mobility (UAM)**

Urban Air Mobility (UAM) is a subset of AAM which refers to efficient and safe air transportation systems within urban areas at lower altitudes (FAA, 2020). It envisions the idea that an air vehicle can replace the automobile in a city environment which can be seen in NASA's UAM concept in Figure (1.1).

According to the NASA Urban Air Mobility Market Study (Goyal, 2018), UAM is viable with a considerable available market value of \$500 billion in the USA alone for a fully unconstrained scenario (Johnson, 2019).



*Figure 1.1* NASA: Urban Air Mobility Concept (NASA, n.d.)

This transportation system can be subdivided into different UAM use cases such as (FAA, 2020):

1. Air taxi
2. Air Ambulance
3. Air Metro
4. Cargo/ Last-mile delivery
5. Recreational / Private use

This new transportation system will consist of an ecosystem that will require the evolution of a myriad of technologies along with infrastructure development and community engagement. The new breed of air vehicles generally take-off and land like a helicopter and transition to winged aircraft during cruise operations. These vehicles can use different aerodynamic configurations like tilt rotor and tilt wing. A typical example of a UAM vehicle is Joby Aviation's aircraft in Figure (1.2).





*Figure 1.2 Joby Aviation's Tilt Rotor Aircraft (Joby, n.d.)*

### **1.3 Distributed Electrical Propulsion (DEP)**

Many UAM vehicles consist of Distributed Electrical Propulsion (DEP) systems. DEP uses multiple electric motors / propulsors for producing aerodynamic thrust (Kim, 2018) which can be seen in Figure (1.3). These thrust producing propulsors do not share a common mechanical power source. In contrast, DEP uses any combination of electrical power generating system (e.g., generator) and/ or energy storage devices as the power sources. The decoupling between propulsive components and power sources resulted in many compact, efficient aircraft configurations as the electrically driven propulsors can be arranged in combination (Kim, 2010).

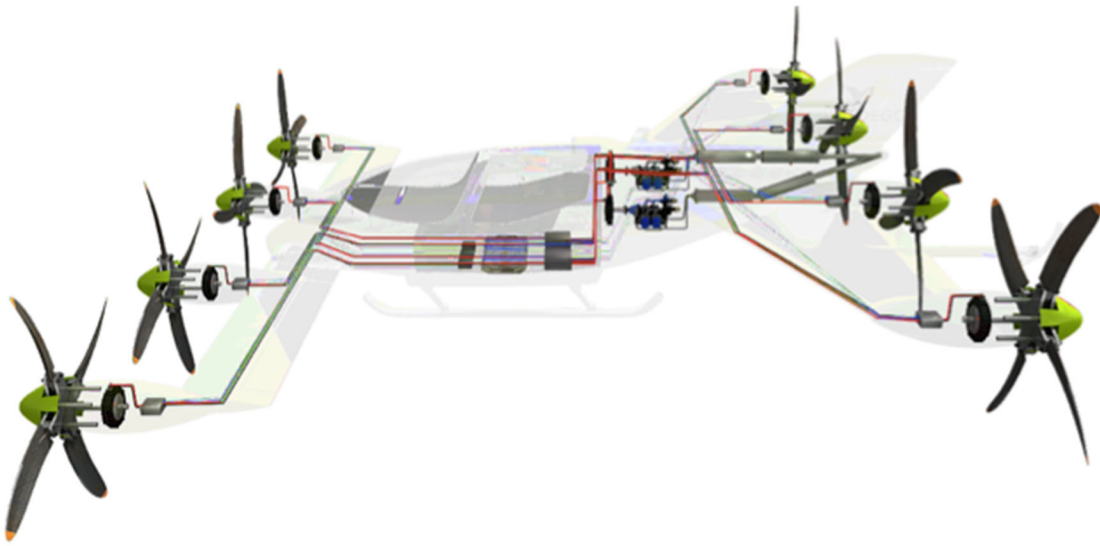


*Figure 1.3* VerdegO Aero: Distributed Electrical Propulsion System (VerdeGo, 2021)

The adoption of DEP systems for air vehicles has resulted in improvements in robustness, capabilities, and overall efficiencies. The thrust generating propulsors can be sized, placed, and operated with better flexibility when compared with a mechanically connected system. Additionally, the distributed propulsive power can be utilized in controlling the air vehicle and reducing dependence on conventional aerodynamic control surfaces. The decoupling of power source and propulsor and coupling of aero propulsion results in better performance over traditional aircraft systems (Kim, 2018).

Furthermore, DEP systems installed with small propulsors provide the ability to leverage acoustic shielding effects (Kim, 2018). This results in a reduced noise signature. The use of DEP systems enhances the operational capabilities with reduction acoustics. The results could make an airplane fly as quietly as an automobile. Therefore, DEP systems can result in significant improvements in future air vehicle designs.

### **1.3. Why Choose Hybrid-Electric Systems for Urban Air Mobility Aircraft?**

With the use of DEP, electric aircraft can support missions which are not possible with a conventional aircraft. The propulsion system of UAM vehicles can be considered as a system with two parts: an electric power source and aerodynamic thrust generation. For the thrust generation, these aircraft use different combinations of propulsors and motors which utilize electrical power to generate the required aerodynamic thrust.

Electric power sources can have different forms. One of the systems that is used is the Energy Storage System (ESS) (Collins, 2021). The plug-in electric batteries used as ESS have the advantage of storing the electric power efficiently produced by the ground power generations units. The stored power can then be used by the aircraft for the airborne operations.

The electric battery system has clear advantages in terms of airborne emissions and fossil fuel consumption. However, the specific energy of the batteries at pack level when compared with the conventional fuel is 1:73 (Collins, 2021; Crabtree, 2015). When an electric battery propulsion system with approximately 75% efficiency is compared with a conventional power plant with approximate thermal of efficiency of 30%, the usable energy ratio remains low at 1:20 (Collins, 2021).

The other potential storage system for electrical energy is hydrogen fuel cells. Hydrogen is the lightest element in the universe and has specific energy approximately three times than that of conventional fuel. The fuels cells have an approximate efficiency of 60%, which is intermediate between conventional gas and batteries (Collins, 2021). However, these systems require heavier fuel tanks and cryogenic temperatures to keep

the hydrogen in a liquid state. These also require significant infrastructure for extraction, storage, and transportation of the hydrogen (Ross, 2006).

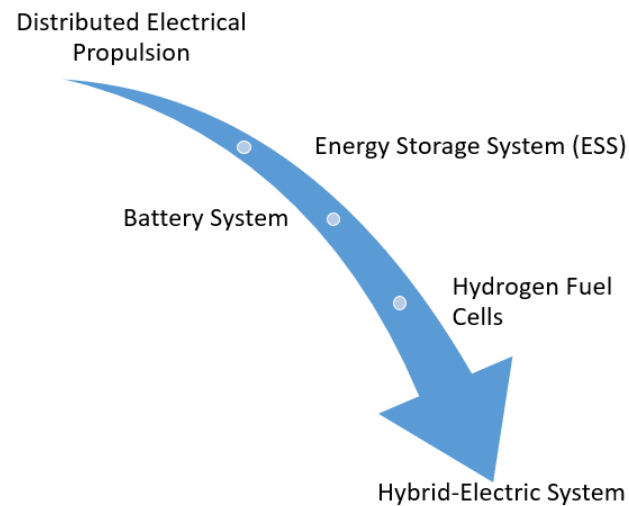


*Figure 1.4* Hybrid Electric System for UAM Aircraft

The hybrid-electric system, which is the combination of a generator connected to a conventional aircraft engine, has evolved as an alternative to fuel cells and batteries, which can be visualized in Figure (1.4) (Lahaji, 2021). These systems have better specific energy when compared with batteries alone and do not require additional infrastructure (Collins, 2021). These systems are generally connected to a small battery pack to complement the energy storing capacity of the system. In addition, the high discharge rate of the batteries can help in augmenting the total power output of the system. The drawback of different ESS, like batteries and hydrogen fuel cells, resulted in hybrid-electric systems as alternative sources of power supply. Hybrid-electric system models can have many benefits, which are discussed in the following section.

### 1.5 Modeling of the Hybrid-Electric System.

Due to limitations of existing battery technology, the hybrid-electric system evolves as a better choice for the power plant for UAM vehicles. The modeling of hybrid-electric systems will assist in design, analysis, verification, and validation of the system. These models can be used to design and support system architectures and requirements from the top level to the system sub-component level. Some of the benefits of the modeling are described in Figure (1.5).

As the hybrid-electric system is a hybrid between an engine and a generator, different design solutions can be analyzed for the mission requirements even before the actual system is assembled. The choice of battery cell and battery pack configuration can be optimized according to UAM aircraft and mission requirements using the developed models without performing experiments.

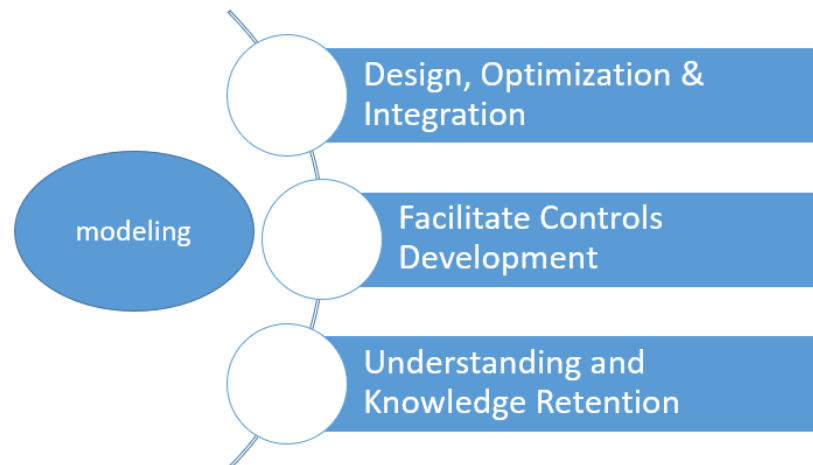


*Figure 1.5* Benefits of Modeling

The models of the hybrid-electric system can aid in the integration of the software and hardware components into a system. These types of testing are generally referred to as hardware-in-the-loop and software-in-the-loop testing. Finally, the models can

effectively provide a means to capture, document and retain the knowledge and understanding of the system. This also helps the evolution of the system to ever changing system requirements to face the emerging needs. Thus, models of hybrid-electric systems have many benefits including the development of control laws. A suitable control law is needed to ensure the system meets desired performance. Therefore, the need for the design of control laws especially for hybrid-electric system is discussed in the following section.

### **1.6. Design of Control Laws for Hybrid-Electric Systems for Urban Air Mobility**

Hybrid-electric systems have been used in the automobile industries for many decades. As a result, control algorithms already exist for hybrid-electric systems in the automotive industry. However, there is a philosophical difference between the automobile and UAM industry. The automobile industry generally considers the cost, fuel efficiency and emission with paramount importance while UAM does consider fuel efficiency as significant, but more importance is given to weight and performance.

The other significant difference between the two industries is the mission/ power requirement. The UAM vehicle may require high power-low energy during the takeoff and landing while these vehicles might also require low power and high energy during the cruise segment of the flight. On the other hand, an automotive vehicle mission depends on the driver, traffic, and the driving conditions. When compared with standardized driving conditions like the Environmental Protection Agency (EPA) Urban Dynamometer Driving Schedule (UDDS), UAM aircraft and automobile vehicles have different mission requirements.

Many UAM vehicles use DEP which might use the propulsor pods to control aircraft performance. Due to the integration of a propulsion system with flight control systems, high frequency control power requirements can exist which are related to flight conditions and are added to quasi-steady power requirements. In general, UAM aircraft have a high base load and a high frequency due to turbulence, while automotive vehicles have a relatively low base load, a low frequency, and a high amplitude due to traffic. As a result, the power requirements of UAM and automobile vehicles are different. Due to the different philosophy as well as different mission and power requirements between the UAM and the automotive industry, the same control strategy might not result in better performance of UAM aircraft. Therefore, a control algorithm which is specially designed for the hybrid-electric system for UAM applications is needed for better overall performance. With the understanding of the importance of modelling of the hybrid-electric system and the need for the development of control laws for hybrid-electric systems, the primary objectives of this thesis can be defined. Thus, the goals of this thesis are discussed in the following section.

### **1.7. Thesis Objectives**

The use of DEP for UAM aircraft and the limitations of existing battery technology result in the evolution of a hybrid-electric system as a suitable alternative electric power source. As a result, there is an increase in the need for models of hybrid-electric systems for UAM aircraft which capture the dynamics of the systems for multiple reasons. The use of hybrid-electric systems also results in the demand for control laws which guide the power plant to meet the UAM aircraft mission requirements. Therefore, there are two primary objectives of this thesis as follows:

- (a) Develop a model of hybrid-electric systems for UAM aircraft.
- (b) Develop control laws for hybrid-electric systems to meet UAM mission requirements.

The development of this thesis can be divided into three stages/ phases, which can be seen in the thesis development overview in Figure (1.6). These three phases helped in achieving the two objectives of the thesis.

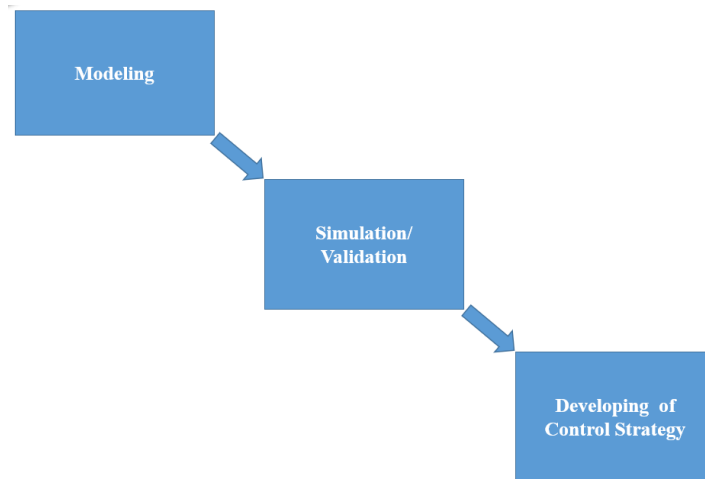


*Figure 1.6* Thesis Development Overview

### **(a) Modeling**

In this phase, the major components of the hybrid-electric system were modeled as idealized electrical elements. Then a free body diagram of the system was created to derive the governing equations. The idealized electrical element model was simulated and then validated using the experimental results to verify the derived governing equations. The verified equations were then used in developing the state-space representation of the hybrid-electric system.



**(b) Simulation /Validation**

In this phase, the developed state-space model was simulated using MATLAB software. Open-loop simulations were performed, and the simulated results were validated with the experimental results. Once the model was able to capture the dynamics of the system, it was used in developing the control strategy.

**(c) Developing Control Strategy**

In this stage, the validated model of the hybrid electric system was used to develop the control strategy to meet the mission requirements of UAM aircraft. The Linear Quadratic Regulator (LQR) was found to be suitable to be used as the controller for the hybrid-electric system. Closed-loop simulations with the LQR controller in the loop with the hybrid-electric plant under constant load with different initial conditions were performed to verify the closed-loop system performance. The model was also used to generate simulation results under a typical UAM power profile. The third phase of development of the control strategy was concluded when the developed LQR controller was able to meet the mission requirements.

The important technologies necessary for the safe operation of UAM, thesis objectives and development phases are discussed in this chapter. Chapter 2 of this thesis will provide the background information and literature review, providing necessary understanding for the thesis, while Chapter 3 will provide information regarding the methodology to achieve the goals of the thesis. The experimental and simulation results are discussed in Chapter 4, followed by discussion and future work in Chapter 5.

## **2. Background and Literature Review**

In this chapter, the necessary background information about different components used in the development of the hybrid-electric system modeled in this thesis is discussed. This chapter also discusses relevant literature like Equivalent Circuit Model (ECM), state-space representation, hybrid-electric control philosophy and other methods which helped in the development of this thesis.

### **2.1 Hybrid Electric Propulsion**

The specific energy of popular the Lithium-Ion Samsung 20s Cell is 0.1 kWh/kg whereas gasoline is 4.09 kWh/kg (Jensen, 2020; Weisstein, 2021). The energy density of batteries must increase to ensure batteries alone can meet longer endurance and range missions for eVTOL. Until battery technology is developed to the level where it can alone meet the energy requirements, hybrid-electric power plants can provide a viable means to meet mission requirements. Therefore, two popular hybrid-electric configurations: serial hybrid and parallel are discussed in the following paragraphs.

A hybrid propulsion system generally consists of an electrical system working in tandem with a mechanical system. The serial hybrid and parallel hybrid configurations have different architectures that define how mechanical and electrical systems interact with each other to generate the power (Finger, 2020). The parallel system consists of a gas engine and electric motor directly connected to the gear box, whereas serial hybrid consists of an electric motor which is driven by batteries and/or a turbine engine via a generator.

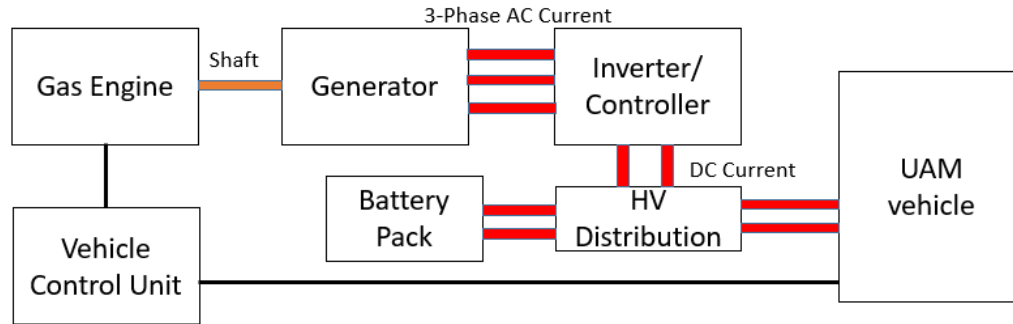


*Figure 2.7* Schematic Diagram of Serial Hybrid Electric System

A schematic diagram of a serial hybrid-electric system is shown in Figure (2.7) as they are suitable for eVTOL operations. The series hybrid-electric system can provide a common electric power source for multiple electric rotors, as many UAM vehicles use Distributed Electrical Propulsion (DEP). The electrical power can be easily supplied and distributed when compared with mechanical shaft power. Therefore, Eagle Flight Research Center (EFRC) at Embry-Riddle Aeronautical University (ERAU) designed, built, and tested a 100 kW serial hybrid-electric system prototype for UAM applications (Collins, 2021).

## 2.2 EFRC's Hybrid-Electric System for UAM Applications

EFRC built a serial hybrid-electric system prototype which can meet the power requirement of UAM aircraft. The prototype built by EFRC is discussed in the following section as it was used to model the hybrid-electric system in this thesis. The assembled system consists of the following major components: ICE, generator, motor controller/inverter, battery pack, and aircraft load / power sink, as shown in Figure (2.8).

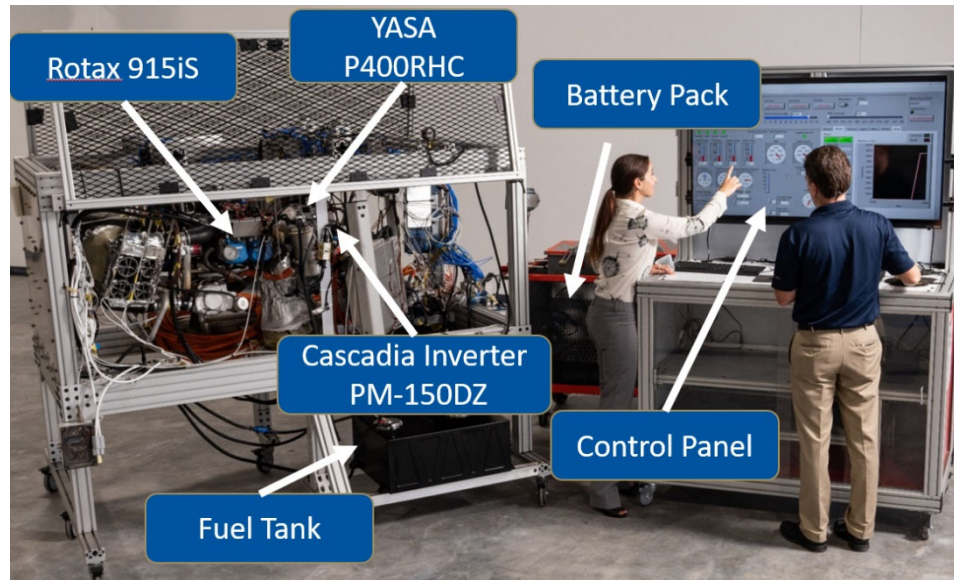


Figure 2.8 EFRC's Serial Hybrid-Electric Power Plant Prototype (Collins, 2021)

The major components of the prototype system are also listed in Table 2.1.

Table 2.1

EFRC's Hybrid-Electric System Components

<b>Engine</b>	Rotax 915iS
<b>Generator</b>	YASA P400RHC
<b>Motor Controller</b>	Cascadia PM-150 DZ
<b>Battery Pack</b>	Samsung 20s Cell (108s 6p)
<b>Aircraft Load / Power Sink</b>	Magna Power WRX100-500-416

The designed system consists of a 4-cylinder turbocharged Rotax 915iS gasoline engine powering the YASA P400RHC. The system also consists of a Cascadia PM-150DZ motor controller and inverter. Additionally, a lithium-Ion battery pack with Samsung 20s cells is also connected in parallel. The load on the power plant is applied using the Magna Power WRX100-500-416. The schematic diagram of the hybrid-electric system is shown in Figure (2.9). The knowledge of the major component used for the

development of the system will help in the modeling of the system. Therefore, major components used for system development are discussed in the following sections.

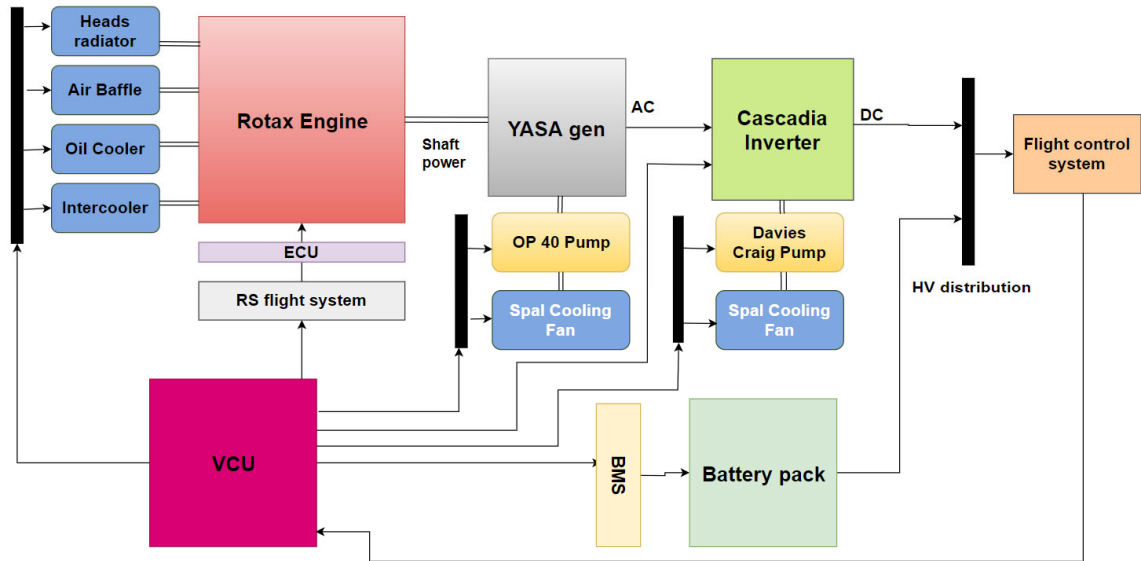


Figure 2.9 Schematic Diagram of Hybrid Electric System

### 2.2.1 Engine

The Internal Combustion Engine (ICE) is the primary source of hybrid-electric power for the UAM vehicle. The important considerations while selecting an engine are power to weight ratio, engine weight and engine speed. A popular aviation gas engine with good power to weight ratio is the Rotax 915 (Rotax, 2021), which was selected by EFRC for the development of the hybrid-electric system shown in Figure (2.10).



*Figure 2.10* Rotax 915 iS Engine (Rotax, 2021)

### **2.2.2 Generator**

The generator selected by EFRC is the YASA P400RHC (YASA, 2021) as shown in Figure (2.11). The generator is the connection between the engine and the remainder of the electrical system. In general, the rated peak power of the generator is limited to a few minutes, and so maximum continuous power is used to measure the performance and suitability. Another important parameter used for the measurement of performance is power to weight ratio. The general trend is the higher the power to weight ratio, the better the generator, especially for a limited weight system.

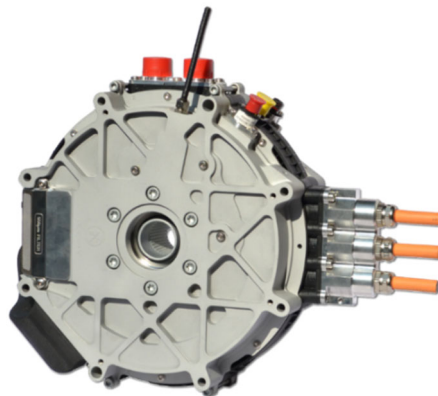


*Figure 2.11* YASA Generator (YASA, 2021)

### 2.2.3 Battery

Batteries are Energy Storage Systems (ESS). Samsung 20s Lithium-ion battery cells (Samsung20s, 2021), shown in Figure (2.12), are arranged in series and parallel combinations to form a custom battery pack. The important characteristics considered while selecting batteries are specific energy density, power density, current limitations, nominal voltage, and total capacity. The battery pack connected to the generator stabilizes the bus voltage of the system by adding capacitance. These systems are used to ensure high power requirements, which are more than the capacity of the generator alone, are met, especially during climb and takeoff. Additionally, in case of emergency, where the generator/engine combination fails, the battery can provide the required power to land safely. These systems also include the Battery Management System (BMS) which ensures the safe operation of the system.



*Figure 2.12* Samsung 20s Battery Cell (Samsung20s, 2021)

### 2.2.4. Vehicle Control Unit (VCU)

dSPACE Microbox II is used as the Vehicle Control Units (VCU) (dSPACE, 2021) as shown in Figure (2.13), which acts like a supervisory controller. The VCU communicates

with different components of the hybrid-electric system to ensure the mission and system requirements are met. In general, the VCU controls the entire system by providing the commanded throttle position to the engine according to the load and SOC (State of Charge) of the battery, which is generally expressed as the percentage of the energy left inside the cell when compared with the available capacity. The system also provides active control to the generator to ensure the generator is in the correct mode according to the mission requirements.



*Figure 2.13* dSPACE Controller (dSPACE, 2021)

### **2.3 Battery Single Cell Equivalent Circuit Model (ECM)**

One of the goals of this thesis is modeling of the hybrid-electric system, which includes modeling of battery pack. A battery pack consists of the battery cell arranged in series and parallel configurations. The modeling of the battery cell will help in modeling of battery pack. A popular method for modeling the battery cell is the Equivalent Circuit Model (ECM) (Huria, 2012) which uses idealized electrical components (Trajković, 2005) and therefore is studied in the following sections.

#### **2.3.1 Idealized Electrical Components**

The analysis of the electrical network can be performed using conceptual electrical elements generally referred to as idealized electrical components. Some of the most



commonly used elements are resistors, capacitors, and inductors, as shown in Figure (2.14). The real physical electrical component is represented by an ideal electrical element. The actual electrical component might not have ideal properties along with non-linearity. The non-ideal behavior of real physical components is modeled using multiple combinations of ideal electrical elements.

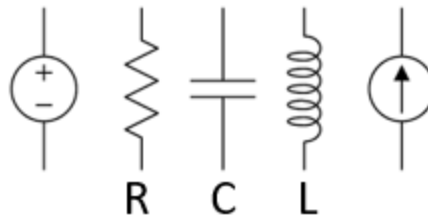


*Figure 2.14* Idealized Electrical Elements

### **2.3.2 Equivalent Circuit Model (ECM)**

The chemical reactions of a battery cell are modeled theoretically using ECM as a non-linear dynamical system. Many ECM models of lithium-ion batteries exist. One of the most used ECM for the Electric Vehicle (EV) applications is the Thevenin Model (Putra, 2015; Lilly, 2017), which is shown in Figure (2.15).

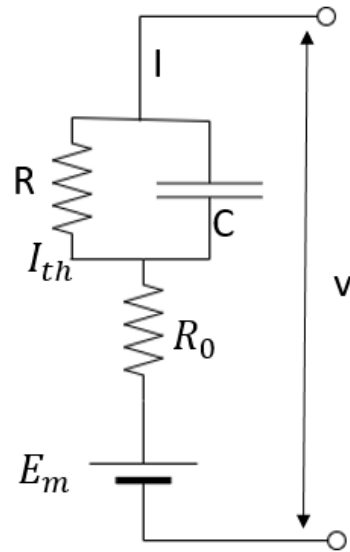


Figure 2.15 Thevenin Model for Lithium-Ion Battery Cell

The Thevenin model for the lithium-ion battery consists of three major parts: open circuit voltage, resistance and a combination of resistors and capacitors (RC) in circuits. The relationship between terminal voltage and current is given in Equations (1) and (2) (Lilly, 2017).

$$V_{RC} = -\frac{1}{RC}V_{RC} + \frac{1}{C}I \quad (1)$$

$$V = E_m - V_{RC} - R_0I \quad (2)$$

where the variables are defined as:

I Current

V Terminal Voltage,

$V_{RC}$  Voltage across RC parallel circuit

#### 2.4 Coulomb Counting Method

SOC is an important parameter to be estimated for the modeling of batteries and a hybrid-electric system as other battery parameters are dependent on the SOC of the cell.

Coulomb counting is a popular method used in the calculation of the SOC of the battery by integrating the discharging current over time. It is the method used to measure the SOC at time (t) from the previously calculated SOC at time (t-1), as shown in Equation (3) (Lilly, 2017; Ng, 2009).

$$SOC(t) = SOC(t - 1) + \frac{I(t)}{Q_n} \Delta t \quad (3)$$

## 2.5 State-Space Representation

A physical system can be modeled using many methods. One of the methods to represent a physical system is state-space representation. The hybrid-electric system can be expressed as a mathematical model using a state-space representation. Therefore, the important fundamentals of state-space models are discussed in the following sections.

The state-space representation has a set of state variables, input and output related by first-order differential equations. The state variables change according to the inputs and time given to the model. These representations can be further divided into Linear Time Invariant (LTI) and Linear Time Varying (LTV) as well as Non-linear Time Invariant and Non-linear Time Varying systems (Brogan, 1991).

The general form of a Linear Time Invariant (LTI) System is based on Equation (4).

$$\begin{aligned} \dot{x} &= Ax + Bu \\ y &= Cx + Du \end{aligned} \quad (4)$$

with the variables and matrices defined as

x - State vector,

y - Output vector,

u - Input vector,

A - State matrix,

B - Input matrix,

C - Output matrix

D - Feedforward matrix.

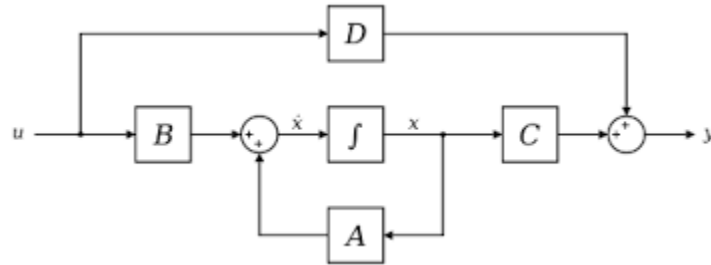


Figure 2.16 Pictorial Representation of State-Space Form

### Linear Time Varying (LTV) system

The Linear Time Varying (LTV) system, also known as a Linear Parameter Varying (LPV) system, is a form of linear state-space model. The dynamics of this system are governed by varying parameters known as the scheduling parameters. LTV systems can be used to capture the non-linear dynamics of the hybrid system by using varying or scheduling parameters. The general form of a LTV system (Brogan, 1991) is given in Equation (5).

$$\begin{aligned}\dot{x} &= A(t)x + B(t)u \\ y &= C(t)x + D(t)u\end{aligned}\quad (5)$$

### State-Space Model with Reference System

The state-space model can be made to track a reference system or reject an unknown disturbance. The state-space model with reference system can be used to model a hybrid-electric system which tracks a reference electric load. The general form of the state-space model tracking the reference system is given in Equation (6).

$$\begin{aligned} \dot{x}(t) &= Ax(t) + Bu(t) + \Gamma u_d(t) \\ y &= Cx \end{aligned} \quad (6)$$

$\Gamma$  – Reference Matrix

$u_d$  - Reference input

The reference input does not necessarily have the same dimensions as the input  $u$ .

### 2.5.1 Stability of System

It is important to analyze the stability of the system. The stability of the hybrid electric system and other important properties like controllability and observability can be analyzed using the concepts of the state-space model. The basic concepts of the stability of linear state-space models which can be applied to hybrid-electric systems are discussed in this section.

The linear system is said to be stable if the states are bounded for the zero-input solution about some equilibrium point. Practically, the system is said to be asymptotically stable if it returns to the equilibrium point after some disturbance (Brogan, 1991). The stability of a linear time invariant system can be evaluated easily using the eigenvalues of the state matrix.

### 2.5.2 Controllability

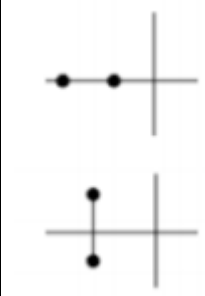
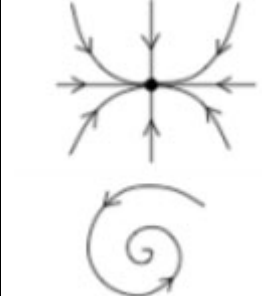


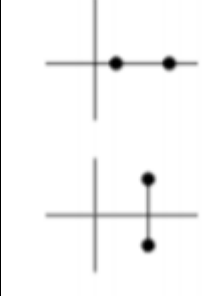
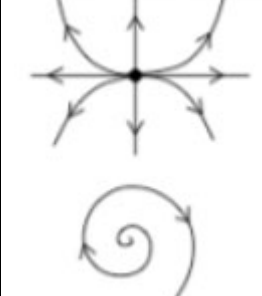
One of the important properties of the control system is controllability. The system is controllable if the states can be changed from any initial condition to any final value using admissible inputs within some finite time. An LTI system is controllable only if the controllability matrix is full rank as seen in Equation (7) (Brogan, 1991).

$$\text{Rank}[B \ AB \ A^2B \ \dots \ A^{n-1}B] = n \quad (7)$$

where  $n$  is the number of states.

Table 2.2

Eigenvalues: Stability of a Linear Time Invariant System

Eigen Value	Eigen Values	Phase-Plane	Stability
(0,2)			Stable
(1,1)			Unstable
(2,0)			Unstable

**2.5.3 Observability**

Another important parameter of a control system is observability. A system is said to be observable if it is possible to estimate the internal states using the external outputs. Controllability and observability are referred to as mathematical duals. Controllability provides information that an input can bring the state to a final desired value from any initial state, while observability provides knowledge if the states of the system can be estimated using output sensors. A system is observable if and only if the observability matrix is full rank, as seen in Equation (8) (Brogan, 1991).

$$\text{Rank} \begin{bmatrix} C \\ CA \\ \vdots \\ CA^{n-1} \end{bmatrix} = n \quad (8)$$

where  $n$  is the number of the states.

## 2.6 Full State Feedback Control

The state-space representation also facilitates the development of the control system. The concepts of modern controls can help in developing the control system of the hybrid-electric system and is therefore studied in this section.

Pole placement or full state feedback control is a control strategy used in feedback control to place the poles of a closed loop plant to a desired location in the  $s$ -plane. The pole of the transfer function of the system are the roots of the characteristic equation in Equation (9) (Brogan, 1991).

$$\det[sI - A] = 0 \quad (9)$$

Therefore, the location of poles of the transfer function are related to eigenvalues of the system, which in turn affects the stability of the system. The input vector can be generated proportional to full state feedback. Therefore, the derived control logic is as in Equation (10):

$$u = -kx \quad (10)$$

where  $k$  is a  $m \times n$  gain matrix.

The control law can be substituted into the state-space equations in Equations (11) and (12).

$$\dot{x} = (A - Bk)x \quad (11)$$

$$y = (C - DK)x \quad (12)$$

The poles of the closed-loop system are calculated as the roots of the characteristic equation in Equation (13):

$$\det[sI - (A - Bk)] = 0 \quad (13)$$

The obtained characteristic equation suggests that the eigenvalues of the closed-loop system can be changed to desired values using the K matrix to obtain the desired system performance (Brogan, 1991). Therefore, if the system is controllable, it can achieve arbitrary eigenvalue placement. The pictorial representation of full state feedback control is shown in Figure (2.17).

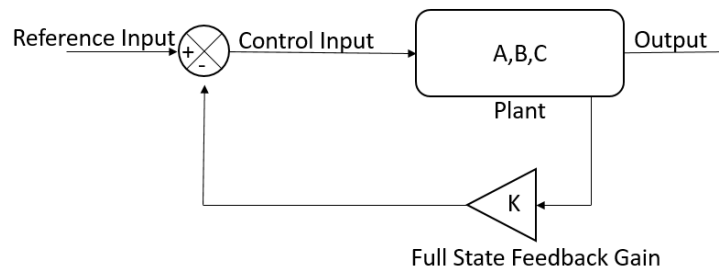


*Figure 2.2 Full State Feedback Control*

## 2.7 Control Philosophy of an Automotive Hybrid-Electric System

Although hybrid-electric systems for the UAM and automotive industries are different, it is necessary to understand the control philosophy of the automotive system. This knowledge can help develop the UAM hybrid-electric control system more effectively. Some of the popular control philosophies of hybrid-electric systems of the automotive industry are discussed in the following section.

As hybrid-electric systems have existed in the automobile industry for many decades (Malikopoulos, 2014), significant work has been done in power management control



algorithms for hybrid-electric automobile vehicles. Some of the developed control strategies for hybrid-electric automobile vehicles are as follows:

- (a) Rule-Based Power Management Control Algorithms
- (b) Offline Power Management Control Algorithms
- (c) Online Power Management Control Algorithms

### **2.7.1 Rule-Based Power Management Control Algorithms**

The primary objective of control of a series hybrid-electric system in the automobile industry is to make sure the engine is operating efficiently while the SOC of the battery is within acceptable limits. A rule-based power management control algorithm can be used to achieve the required control objectives. The strategy used in these algorithms is to split the power demand between the batteries and the engine in such a way that the two power sources operate at the highest efficiency (Jalil, 1997).

The power required by the automobile is calculated using the vehicle's longitudinal acceleration. The power assignment (split) between the engine and battery is done using a rule-based frame to improve the fuel economy of the vehicle. The power split depends on the various selected variables such as:

1. Driver's acceleration command
2. Power demand
3. SOC of the battery

The power assignment rule ensures the high efficiency between the engine and batteries whenever possible.

### **2.7.2 Offline Power Management Control Algorithms**

Offline Power Management Control Algorithms are used to find the optimal control for dynamic systems. The control problem is based on sequential decision making where the controllers are tasked to perform different actions in certain time steps to achieve the long term goals of maintaining the system efficiency (Lin, 2003). These sequential decisions are modeled mathematically, and each decision is made in different steps, incurring a cost at each state. An important aspect of this problem is that each decision made influences the future decisions (Wang, 2007). The total time under which the system performance is observed is called the decision-making horizon (Malikopoulos, 2014).

#### **Dynamic Programming**

Dynamic Programming (DP) is widely used as the analysis method for sequential decision-making problems. This method can be employed in different decision-making problems as the underlying structure is essentially same, with two distinct features (Bertsekas, 2007) :

1. Discrete-time dynamic system
2. Cost function

The primary objective of DP is to derive optimal logic that can minimize the optimization criteria and is based on the principal of optimality. “An optimal policy has the property that whatever the initial state of the system and initial decision are, the remaining decisions must constitute an optimal policy with regards to the state resulting from the first decision” (Bertsekas, 2007; Bellman, 1957).

While DP can provide an optimal solution globally, the required computations for the optimization problem are overwhelming. Additionally, the complete solution for many problems might not exist. The computation requirements increase exponentially as the problem size increases and is referred to as the “curse of dimensionality” (Bellman, 1957). In general, DP is considered a rigorous approach for sequential decision-making problems.

### **2.7.3 Online Power Management Control Algorithms**

Offline power management control algorithms like DP can yield optimal solutions to complex problems; however, the excessive computational requirements restrict implementation in UAM vehicles. These control policies can grow their complexity exponentially as the size of the problem increases. To address these problems, online power management control algorithms have been developed. These algorithms are generally associated with self-sustainability and very little knowledge of future condition. The online power management control algorithms which are popular and commonly used are Model Predictive Control (MPC) and Equivalent Fuel Consumption Minimization Strategy (ECMS).

#### **Model Predictive Control**

Model Predictive Control (MPC) obtains required control actions by formulating and solving the optimization online for problems over a small horizon. In MPC, the control solution is calculated by solving an iterative optimization of the plant model over a finite horizon using a cost function (Ripaccioli, 2010). MPC is generally not recommended for a system with fast dynamics. This method is mostly used for systems with slow dynamics

with sample time calculated in minutes and seconds. There are examples of MPC for vehicles with faster dynamics, however.

### **Equivalent Fuel Consumption Minimization Strategy (ECMS)**

The Equivalent Fuel Consumption Minimization Strategy is one of the popular strategies of Hybrid-Electric Automobile vehicles. These control policies provide fast and instantaneous optimal control solutions and are computationally efficient. In this method, Energy Storage Systems like super capacitor /battery packs are considered as buffered energy sources. The equivalent energy consumption of an Energy Storage System is calculated as fuel consumption and electric power consumption cannot be compared directly (Gao, 2009). A cost function containing the fuel consumption of electrical energy consumption and ICE is formed. The obtained cost function is minimized to calculate the optimal control policy.

### **2.8 EFRC's Hybrid-Electric Load Following Controller for UAM Applications**

EFRC developed a load following controller for the hybrid-electric system to meet the mission requirements of UAM aircraft (Collins, 2021). It will be helpful to understand the developed load following controller as one of the goals of this thesis is to develop the control system for the same hybrid-electric system.

Classical control methods were applied by EFRC to the hybrid-electric system to meet the mission requirements of the UAM. The control logic of feedforward and feedback controls are used in the hybrid-electric power plant controller. As the two primary requirements are power requirements and SOC management, the control strategies are based on feedforward control, which ensures the required electrical power is generated according to the load, and feedback control, which improves the accuracy of

the controller and manages the SOC (Lahaji, 2021). The fundamental architecture of the developed control law by EFRC consisting of feedforward and feedback control as well SOC management control are discussed in the following sections.

### 2.8.1 Feedforward Control

The feedforward logic receives required load power as the input. The algorithm calculates the desired torque to be generated by the engine to achieve the required load power. The load power,  $L(t)$ , is divided by the combined generator and inverter electrical efficiency ( $\eta$ ) and speed ( $\omega$ ) to obtain the feedforward torque, as shown in Equation (14).

$$T_t = \frac{L(t)}{\eta * \omega} \quad (14)$$

This process does not check the effectiveness of the control input and is not self-correcting. Therefore, feedback control is also used in conjunction with feedforward control as shown in Figure (2.18).

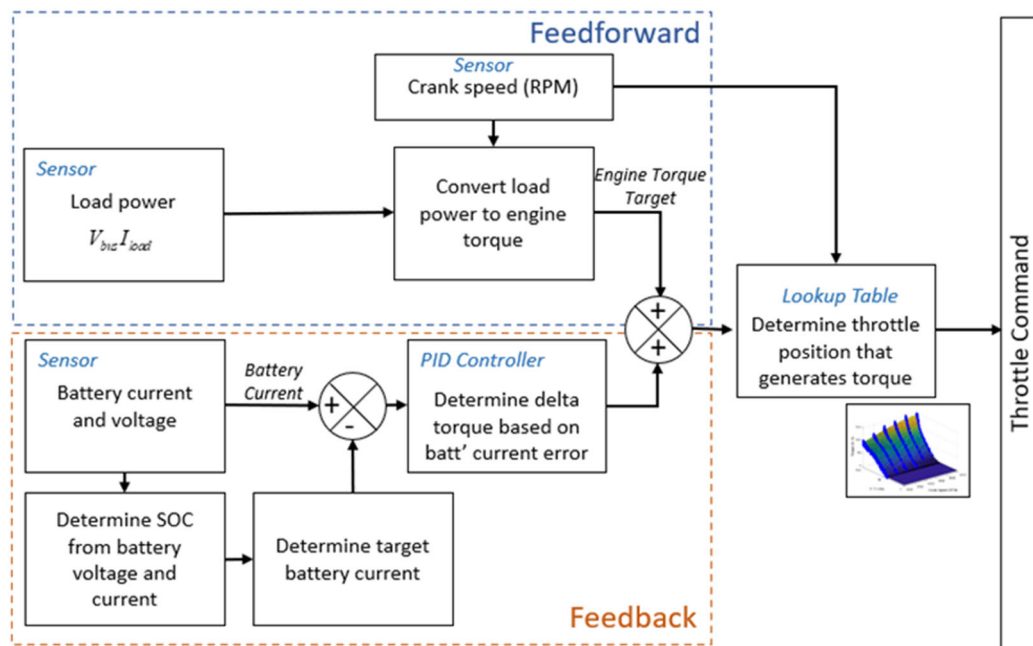
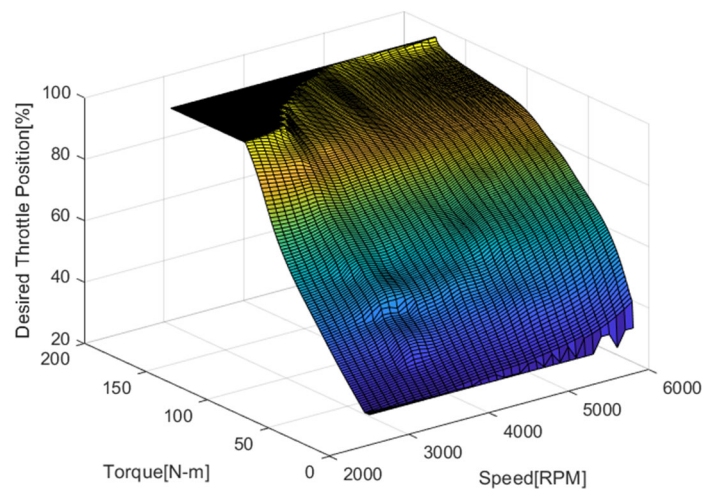


Figure 2.18 EFRC's Feedforward and Feedback Control

### 2.8.2 Feedback Control

The feedback control is based on the battery current. The required data of battery current are obtained from the battery sensors. The SOC management algorithm provides the target current. The error between the actual current and the target that was calculated is used as an input to a PI controller. The PI controller with dynamic saturation and back stepping is used to avoid commanding torques that exceed the engine's capability and to avoid integral windup. This computation provides an estimated torque needed from the engine.

The total torque needed from the engine is then the sum of both the feedforward torque estimate and the torque estimate obtained from the feedback PID controller. The engine throttle required to produce the total torque is obtained from a lookup table, the data of which are shown in Figure (2.19). The lookup table provides the desired throttle position for the given torque and speed of the generator. The data in the table were generated from dynamometer testing of the ICE and converts the torque into the corresponding throttle position.



*Figure 2.3* Data to Determine the Desired Throttle Position for Torque and Speed

### 2.8.3 SOC Management

The SOC of the batteries is maintained through a SOC management algorithm. The system selects a target current through a lookup table and target SOC specified by the user, as shown in Figure (2.20).

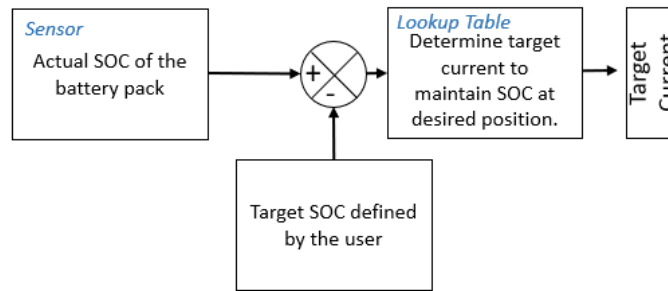


Figure 2.4. SOC management control logic

The magnitude and direction of the target current depends on the error between target SOC and actual SOC considering a C-rate limit to mitigate excessive heating of the batteries (Collins, 2021). The target current is calculated using the lookup table data shown in Figure (2.21).

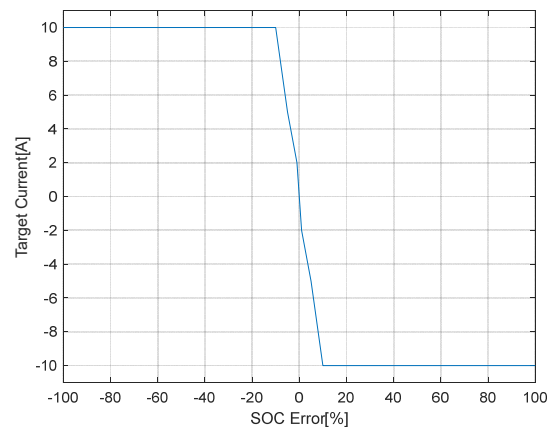


Figure 2.5 SOC Management: Target Current Lookup Table

This output is saturated on the low end if the current engine speed is within 100 rpm of idle speed to prevent lugging of the engine at idle. The upper end is saturated by a curve that decreases to zero at maximum allowed battery voltage to prevent inadvertent overcharging of the battery.

The classical control logic employed by EFRC, along with other relevant literature as well as the necessary background information, was discussed in this chapter. The performance of classical control methods may be improved by using concepts of modern control, especially in tracking hybrid-electric system states like SOC without steady state error. The concepts of optimal control can also be applied to increase the efficiency of the system. Therefore, modern control theory was applied to the hybrid-electric system of the UAM vehicle, which is discussed in Chapter 3 of this thesis. The methodology used in the development of models of the hybrid-electric system is also discussed in Chapter 3.



### 3. Methodology

This chapter discusses the methodology used for the modeling of the hybrid-electric system followed by the derivation of governing equation of state-space model. The controls requirements, developed LQR controller, and simulation codes of different models are also discussed in this chapter.

#### 3.1. Modeling of Hybrid-Electric System using Idealized Electrical Components

The different components of the hybrid-electric system, like the generator, battery pack and load, can be modeled as idealized electrical elements under some desired condition. The assumed idealized electrical elements for the sub-systems can then be used to create a free body diagram and then derive the differential equations governing the major components. MATLAB/ Simscape software provides the flexibility to model the system directly using the electrical elements. This helps in modeling a non-linear system by defining the constants used in the idealized electrical elements.

Additionally, the derived differential equations which govern the dynamics of the system can be linearized /simplified and used to model a linear state-space model of the hybrid-electric system.

##### 3.1.1. Internal Combustion Engine (ICE)

The Rotax 915iS is an aviation gasoline engine used by EFRC for the development of the hybrid-electric system. It generates the mechanical energy by burning fuel. The input to the engine is throttle position ( $u_{th}$ ) and the outputs are torque and RPM of the shaft. The relationship between the actual throttle position and torque is obtained from the experimental results and is found to be non-linear, as shown in Figure (3.22). However, to simplify the engine modeling, within a certain region as shown in Figure (3.23), the

steady state torque ( $T_{ss}$ ) is assumed to be a linear function of throttle/ percentage of power with  $\alpha_1$  as the proportionality constant, as shown in Equation (15), and RPM is considered constant.

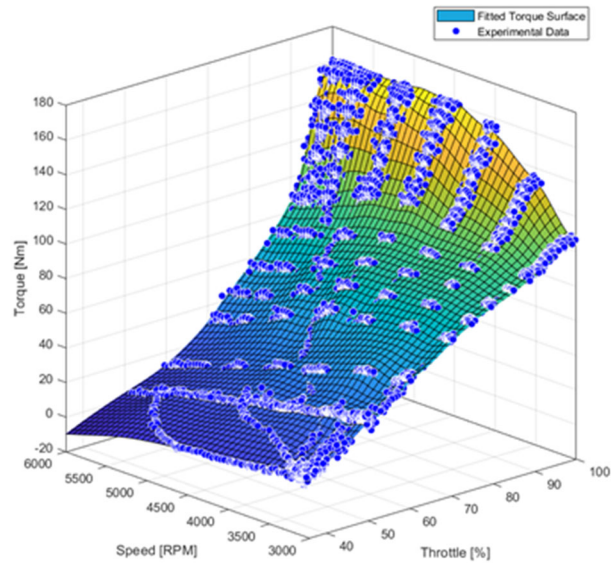


Figure 3.6 Rotax Torque-Speed-Throttle Map

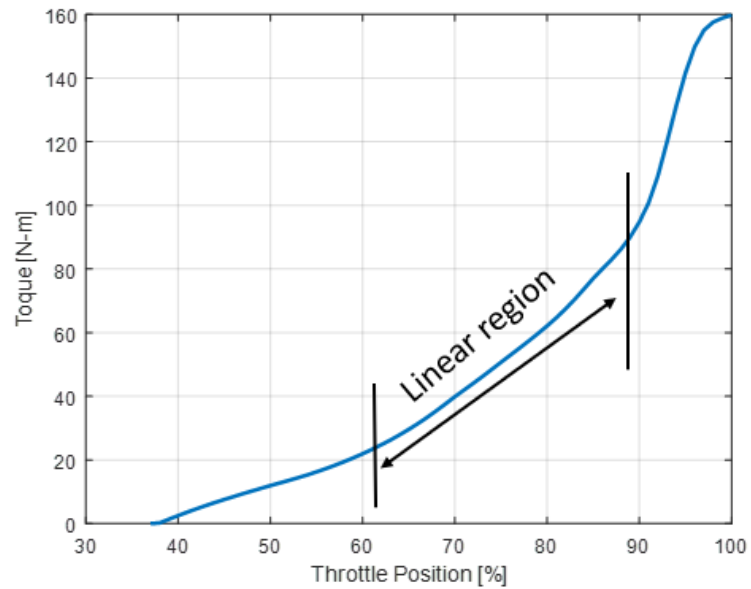


Figure 3.7 Rotax Engine Torque vs Throttle Map at 5500 RPM

Therefore, the torque at a steady state generated by the engine is modeled using Equation (15).

$$T_{ss} = \alpha_1 * u_1 \quad (15)$$

Furthermore, as the engine is a mechanical system, it is observed that there is delay in the engine response to change in throttle. Therefore, to model the engine torque ( $T_t$ ) at time  $t$ , a first-order lag equation with  $\tau$  as the time constant is used as shown in Equation (16).

$$\tau \left[ \frac{dT}{dt} \right] + T_t = T_{ss} \quad (16)$$

The torque equation is transformed into the Laplace domain to model the engine as a transfer function in Equation (17).

$$T_t = \frac{\alpha_1}{\tau s + 1} u_1 \quad (17)$$

### 3.1.2 Generator/Inverter

A YASA P400RHC motor is used to generate AC current and can act as a motor or generator based on the direction of torque and current. The Cascadia PM 150 is used to convert the AC current, which is produced by the generator, to DC current. Moreover, the inverter also controls the motor by keeping the generator in different modes: speed mode and torque mode. However, for the purpose of modeling, the generator and motor controller are modeled as a single unit. The performance of the combined generator and inverter is shown in Figure (3.24).

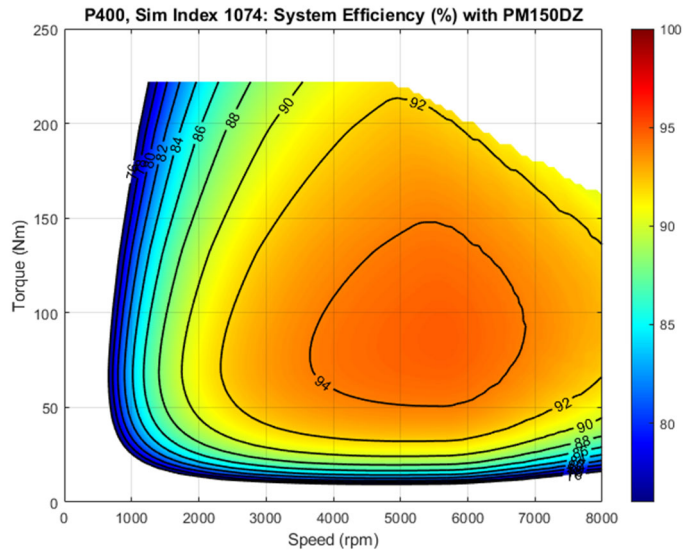


Figure 3.8 YASA Generator and Cascadia Combined Efficiency Map

It can be considered that the input to the generator system is mechanical power in terms of torque and speed, and output is electrical power in the form of current and voltage. During the operation and testing, the subsystem is mostly used in speed mode in order to maintain the desired constant speed and achieve better overall efficiency. In addition, the bus voltage of the system mainly depends on the terminal voltage of the battery pack. As the generator speed is considered as constant, and the voltage of the system is mainly dictated by the battery pack terminal voltage, the input to generator can be considered as torque and output as generator current.

Therefore, the electric current generated by the generator/ inverter combination is assumed to be proportional to torque ( $T_t$ ) whereas  $\alpha_2$  is the proportionality constant designated as the generator constant, as shown in Equation (18).

$$i_g = \alpha_2 T_t \quad (18)$$

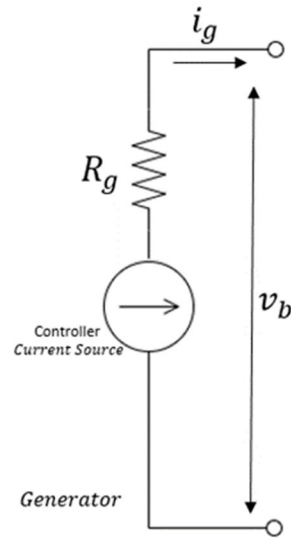


Figure 3.9 Generator/ Inverter Variable current source with some internal resistance

The generator/inverter combination is modeled as a variable current source as shown in Figure (3.25).

### 3.1.3. Battery Pack

EFRC has designed a custom battery pack consisting of lithium-ion cells arranged in the configuration of 108 cells in series and 6 cells in parallel, which is generally referred to as the 108S 6P configuration. The Samsung 20s power cell was selected for the development of the battery pack. The battery pack nominal voltage is 388V whereas the capacity is 4.5kWh. The battery pack of the system can be modeled using the model of the battery cell. The model of the battery cell is then scaled to the battery pack using gains according to the battery pack configuration.

The battery cell parameters which are of most interest are battery terminal voltage, battery current and SOC. The battery cell open circuit voltage ( $v_{oc}$ ) can be used in calculating the terminal voltage and is a function of SOC (Hurria, 2012). The relationship between  $v_{oc}$  and the SOC is given in Equation (19). The constant  $a_0$  is the terminal

voltage of the battery at when SOC is zero and  $a_1$  which is determined using  $a_0$  and  $V_{oc}$  at maximum SOC.

$$V_{oc} = a_1 * SOC(t) + a_0 \quad (19)$$

The battery is modeled as the combination of voltage source and internal resistance in series. The battery terminal voltage is given by Equation (20).

$$V_b = V_{oc} + V_r \quad (20)$$

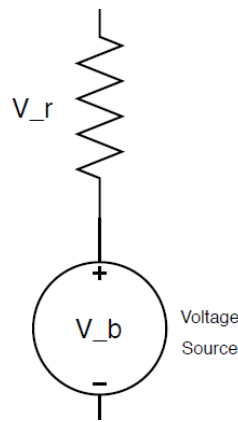


*Figure 3.10* Modeling of battery as variable voltage source

The voltage across the battery internal resistance is found using Ohm's law, where  $a_2$  is internal resistance as shown in Equation (21).

$$V_r = a_2 i_b \quad (21)$$

Therefore, the battery terminal voltage  $V_b$  is found to be a linear function of the SOC and current within a region, as shown in Figure (3.27), obtained from Lygte-info (Jensen, 2020).

$$V_b = a_1 * SOC(t) + a_2 * i_b + a_0 \quad (22)$$

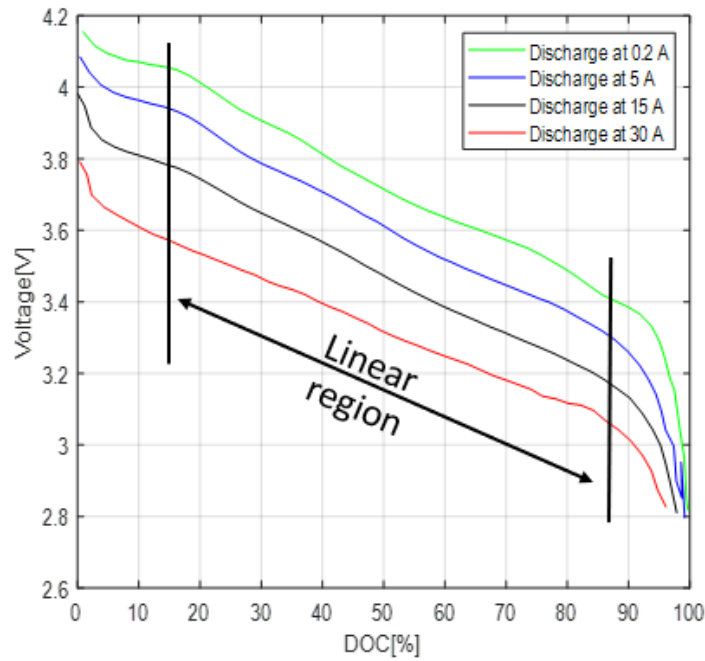


Figure 3.11 Experimental Results of Discharge Test of Samsung 20s Battery Cell

The SOC of the battery is calculated using the Coulomb counting method (Lilly, 2017) using Equation (23).

$$SOC = \frac{i_b}{Q_n} \quad (23)$$

The battery current is modeled using the relationship shown in Equation (24) obtained from Kirchhoff's Current Law, as the battery pack is connected within the circuit.

$$i_b = i_g - i_l \quad (24)$$

### 3.1.4 Aircraft Load / Power Sink

The electrical current generated by the hybrid system is utilized by the aircraft. To model the aircraft power requirement, a load sink is created. A Magna Power WRX100-500-416 active load is used to generate the electrical load for the hybrid-electric power

plant. This electrical load is modeled using a variable resistor, as shown in Equation (25) and Figure (3.28).

$$L = i_l^2 R_l(t) \quad (25)$$



Figure 3.12 Modeling of Aircraft load as variable resistor

The load power is governed by the following electrical power and Ohm's Law, and the bus following equation is obtained as shown in Equation 26.

$$i_l = \frac{V_b}{R_l(t)} \quad (26)$$

### 3.1.5 Free-body Diagram of Hybrid-Electric System

A free body diagram of the hybrid-electric system is created using the derived mathematical equations of engine, generator system, battery pack and power sink.

Table 1.3

Hybrid Electric Components Represented as Idealized Electrical Elements

ICE	Transfer Function
Generator/Inverter	Variable Current Source, Resistance
Battery Pack	Variable Voltage Source, Resistance
Power Sink	Variable Resistance

The internal combustion engine (ICE) of the system is modeled using a transfer function while the generator/inverter is modeled as a variable current source with some internal resistance. The battery pack is modeled as variable voltage source with some internal



resistance in series. The load is modeled as a variable resistance as shown in Figure (3.29).

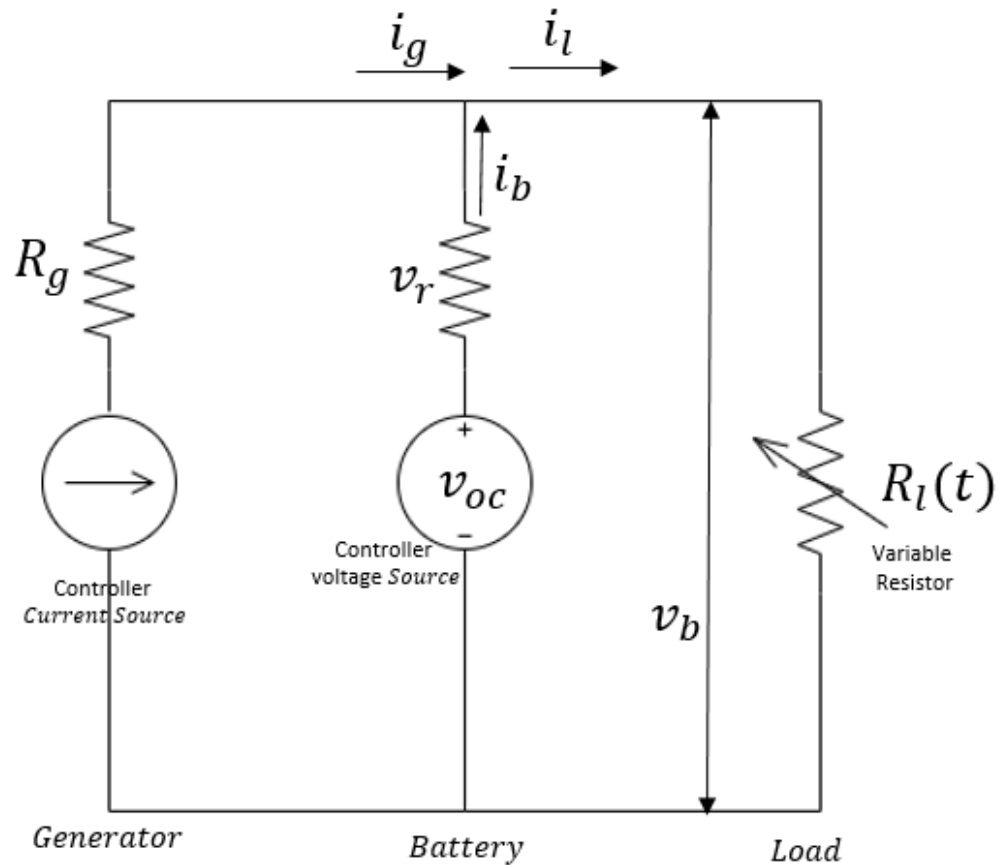


Figure 3.13 Free Body Diagram of Hybrid Electric System

### 3.2. Modeling of the System using State-Space Representation

The state-space representation of the hybrid electric system will facilitate the analysis of the system and will help in the control logic development. A Linear Time Varying (LTV) system was used to model the hybrid electric system to capture the non-linear dynamics of the bus voltage.

The important parameters of the hybrid-electric system are engine torque, shaft speed, generator current, battery current, bus voltage, SOC of the battery pack and load current.

The engine torque and SOC of the batteries are chosen as the states, while bus voltage is chosen as the variable parameter of the LTV system.

### 3.2.1 Derivation of State Differential Equations

#### Torque State

The torque state of the system is derived like the torque equation in the idealized element model. The steady state torque is assumed to be a linear function of throttle, and the delay in the response of the engine system is captured using a first order lag equation (28).

$$T_{ss} = \alpha_1 * u_1 \quad (27)$$

$$\tau \left[ \frac{dT}{dt} \right] + T_t = T_{ss} \quad (28)$$

The above equations are rearranged to find the torque state of the state-space model of the hybrid-electric system in Equation (29).

$$\dot{T} = \frac{\alpha_1}{\tau} u_1 - \frac{T_t}{\tau} \quad (29)$$

#### State of Charge (SOC) State

To derive the SOC state of the system, the relationship between SOC and battery is used from the Coulomb counting method as in Equation (30).

$$SOC = \frac{i_b}{Q_n} \quad (30)$$

As the battery system is connected to the generator and load in the electrical circuit, the Kirchoff current law is used to find the battery current in terms of generator and load current as seen in Equation (31).

$$i_b = i_g - i_l \quad (31)$$

Equation (31) is then substituted into Equation (30), resulting in Equation (32).

$$S\dot{O}C = \frac{1}{Q_n} [i_g - i_l] \quad (32)$$

The current generated by the generator and inverter combination is assumed to be a linear function of the torque. The relationship between torque and generator current is modeled as in Equation (33).

$$i_g = \alpha_2 T_t \quad (33)$$

The assumed relationship is substituted into the SOC relationship, from which the following relationship is obtained in Equation (34):

$$S\dot{O}C = \frac{1}{Q_n} [\alpha_2 T_t - i_l] \quad (34)$$

The load current can be expressed in terms of load  $L$  and bus voltage using the power equation as in Equation (35):

$$i_l = \frac{L}{v_b(t)} \quad (35)$$

The load current relation is then substituted into the SOC equation to obtain the following equation:

$$S\dot{O}C = \frac{1}{Q_n} [\alpha_2 * T - \frac{L}{v_b(t)}] \quad (36)$$

This equation can be re-arranged to obtain the SOC state equation.

$$S\dot{O}C = \frac{\alpha_2}{Q_n} T - \frac{1}{Q_n v_b(t)} L \quad (37)$$

### 3.2.2 Derivation of the Variable Parameter: Bus Voltage

The bus voltage of the hybrid electric system is stabilized and maintained by the battery terminal voltage. From Figure (27), the battery terminal voltage is found to be a function of SOC and battery current as in Equation (38):

$$V_b = f(SOC) + g(i_b) \quad (38)$$

The experimental results suggest that, in some desired region, the battery terminal voltage can be modeled as a linear function of SOC and battery current. The battery relationship is shown in the equation with  $a_0$  as terminal voltage of the battery at SOC equal to zero and  $a_1$ , which is determined using  $a_0$  and battery open circuit voltage at maximum SOC.

$$V_b = a_1 * SOC(t) - a_2 * i_b + a_0 \quad (39)$$

The bus voltage equation can be further modified using the SOC and battery current equations.

$$V_b = a_1 SOC(t) - a_2 Q_n \dot{SOC} + a_0 \quad (40)$$

### 2.2.3 State-Space Representation of Hybrid-Electric system

The torque and SOC state equations are modeled using an LTV state-space representation with reference system and bus voltage as the variable parameters. The derived state equation of the hybrid-electric system takes the form of Equation (41).

$$\dot{x}(t) = Ax(t) + Bu(t) + \Gamma u_d(t) \quad (41)$$

$$\begin{bmatrix} \dot{T} \\ \dot{SOC} \end{bmatrix} = \begin{bmatrix} \frac{-1}{\tau} & 0 \\ \frac{\alpha_2}{Q_n} & 0 \end{bmatrix} \begin{bmatrix} T \\ SOC \end{bmatrix} + \begin{bmatrix} \frac{\alpha_1}{\tau} \\ 0 \end{bmatrix} [u^{th}] + \begin{bmatrix} 0 \\ \frac{-1}{Q_n * v_b(t)} \end{bmatrix} [L]$$

The output vector equation of the hybrid-electric system is given in Equation (43).

$$y = Cx \quad (42)$$

$$\begin{bmatrix} T \\ SOC \end{bmatrix} = \begin{bmatrix} 1 & 0 \\ 0 & 1 \end{bmatrix} \begin{bmatrix} T \\ SOC \end{bmatrix} \quad (43)$$

The variable parameter of the system is given by the following Equation (44):

$$V_b = a_1 SOC(t) - a_2 Q_n \dot{SOC} + a_0 \quad (44)$$

In summary, the state-space matrices of the system are as follows:

$$\dot{x}(t) = \begin{bmatrix} \dot{T} \\ \dot{SOC} \end{bmatrix}, A = \begin{bmatrix} \frac{-1}{\tau} & 0 \\ \frac{\alpha_2}{Q_n} & 0 \end{bmatrix}, B = \begin{bmatrix} \alpha_1 \\ \tau \\ 0 \end{bmatrix}, \Gamma = \begin{bmatrix} 0 \\ -1 \\ Q_n * v_b(t) \end{bmatrix}, y = \begin{bmatrix} T \\ SOC \end{bmatrix}, C = \begin{bmatrix} 1 & 0 \\ 0 & 1 \end{bmatrix}$$

The other important parameters of the hybrid-electric system, that is, generator current, battery current and load current, are given as follows:

$$i_g = \alpha_2 T_t \quad (45)$$

$$i_l = \frac{L}{v_b(t)} \quad (46)$$

$$i_b = \alpha_2 * T - \frac{L}{v_b(t)} \quad (47)$$

Table 4.4

Governing Equations of Hybrid Electric System

Components	Governing Equations	Constants
Engine	$T_{ss} = \alpha_1 * u_1$ $\dot{T} = \frac{1}{\tau} [\alpha_1 * u_1 - T_t]$ $T_t = \frac{\alpha_1}{\tau s + 1} u_1$	$T_t$ – Torque at time(t) $T_{ss}$ – Torque at Steady state $\tau$ – Time constant $\alpha_1$ – Engine Constant = $\frac{T_{ss}}{u_1}$ $u_1$ – Power percentage
Generator	$i_g = \alpha_2 T_t$	$\alpha_2$ – Generator Constant = $\frac{i_g}{T_{ss}}$ $i_g$ – Generator Current
Battery	$V_b = a_1 * SOC(t) - a_2 * i_b + a_0$ $V_b = a_1 SOC(t) - a_2 Q_n \dot{SOC} + a_0$ $\dot{SOC} = \frac{i_b}{Q_n}$ $i_b = i_g - i_l$	$i_b$ – Battery Current $i_l$ – Load Current $V_b$ – Battery Terminal Voltage $V_{oc}$ – Battery Open Circuit Voltage $a_1$ – SOC Constant $a_2$ – Battery Current Constant $Q_n$ – Battery Capacity $a_0$ – Battery Constant

### 3.2.4 Analysis of State-Space Model of Hybrid-Electric System

The state-space model of the hybrid-electric system is helpful in analyzing the system. The properties of the open-loop hybrid-electric system, such as stability, controllability and observability, have been analyzed.

**Stability of the system:** The Lyapunov indirect method was applied to the linear time varying hybrid-electric state-space model. The eigenvalues of the state matrix are found to exist with real part as positive. Therefore, according to the Lyapunov indirect method analysis, the system is unstable.

$$\text{Eigen values}(A) = \text{Eigen Values} \left( \begin{bmatrix} \frac{-1}{\tau} & 0 \\ \frac{\alpha_2}{Q_n} & 0 \end{bmatrix} \right)$$

**Controllability:** As the hybrid-electric system is found to be unstable, the system states can be changed from any initial condition to the final desired states if and only if the system is controllable. The controllability of the system is found using the rank of the controllability matrix. The controllability matrix is full rank, from which it is concluded that the system is controllable.

$$\text{Rank}[B \ AB] = n$$

$$\text{Rank} \left[ \begin{bmatrix} \alpha_1 \\ \tau \\ 0 \end{bmatrix} \quad \begin{bmatrix} \frac{-1}{\tau} & 0 \\ \frac{\alpha_2}{Q_n} & 0 \end{bmatrix} * \begin{bmatrix} \alpha_1 \\ \tau \\ 0 \end{bmatrix} \right] = n$$

**Observability:** Another important property of the system is observability. The observability of the system is found using the rank of the observability matrix. The observability matrix is found to be full rank, which concludes the system is observable.

$$\text{Rank} \begin{bmatrix} C \\ CA \end{bmatrix} = n$$

$$\text{Rank} \left[ \begin{array}{cc|cc} 1 & 0 & & \\ 0 & 1 & & \\ \hline 1 & 0 & \begin{array}{c} -1 \\ \tau \end{array} & 0 \\ 0 & 1 & \begin{array}{c} \alpha_2 \\ Q_n \end{array} & 0 \end{array} \right] = n$$

### 3.3 Controls Requirements of the Hybrid Electric System for UAM Applications

The hybrid-electric power plant is designed to meet the power requirements of UAM aircraft. As UAM aircraft have different mission requirements, the controller must ensure all the requirements are met. The two important controls requirements of the hybrid electric power plant are as follows:

- (a) Mission power requirement
- (b) SOC management requirement

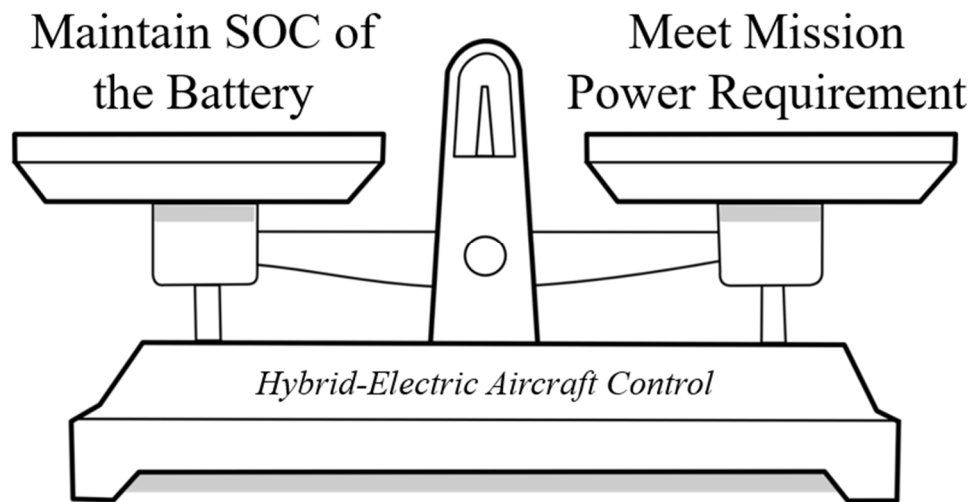
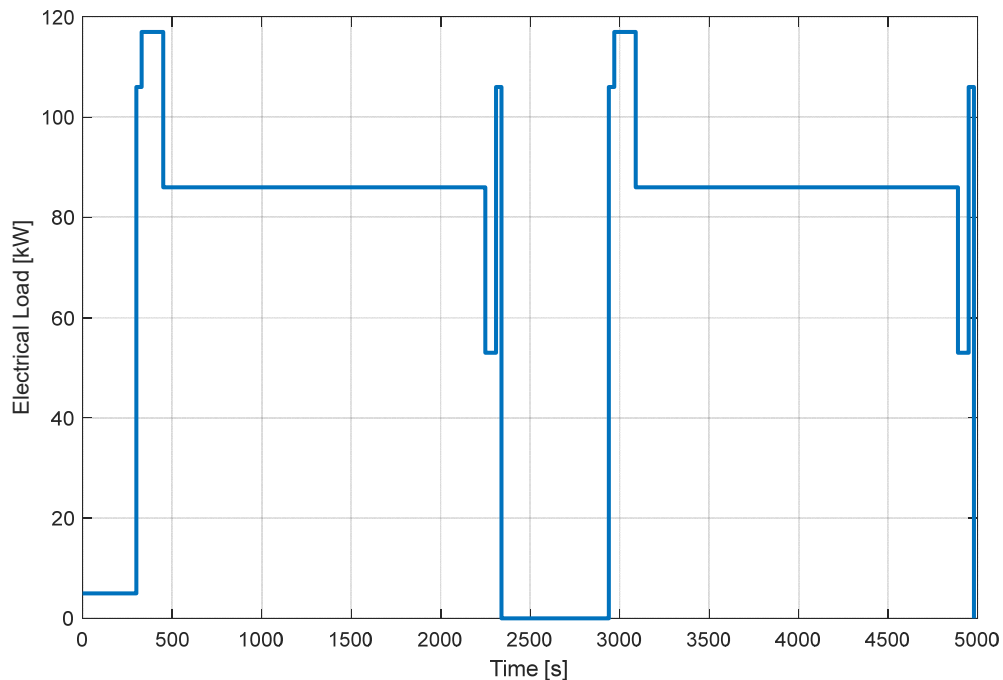


Figure 3.14 Control Requirement of Hybrid-Electric System

The controller is required to balance between the two primary control requirements as shown in Figure (3.30).

### 3.3.1 Mission Power Requirement

The primary controls requirement of the hybrid electric system is to ensure that the power/load requirement of the UAM mission is met. As the hybrid electric system has two power sources, engine-generator power and battery power, the control system has to ensure the power generation and supply are balanced between the generator and battery pack. The UAM aircraft power requirement changes according to the mission segment. For example, high power is required during take-off and landing, while cruise and descent are generally accompanied by lower power requirements. The power requirement of a typical UAM aircraft is shown in Figure (3.31).



*Figure 3.15* Power Requirement of Typical UAM Aircraft

The hybrid electric system built by EFRC is configured in such a way that most of the mission power requirements should be met by the engine-generator power. The battery



power source is designed to supply power only when the power requirement of the system exceeds the capacity of the engine- generator. The battery power system is also utilized by the UAM in case of emergency when the engine-generator system fails. Therefore, the control system should ensure that all the power requirements of the UAM aircraft are met using the engine generator system during normal operations, while battery system power usage is minimum and is utilized only during emergency operations.

### **3.3.2 SOC Management Requirement**

The other important requirement of the control system is to ensure that the SOC of the battery pack is maintained at a desired level. The bus voltage of the system is generally dictated by the terminal voltage of the battery pack, which is in turn dependent on the SOC of the batteries. Thus, it is necessary to maintain the SOC at some desired set point to ensure desired bus voltage. The other important reason to maintain SOC is for emergency backup power. The SOC of the battery pack is a measure of energy stored in the battery system. As a result, higher SOC is desirable to ensure sufficient energy is always available to the system to safely land in case of any failure. Therefore, the controls systems have to ensure that the SOC of the battery pack is maintained at some desired point.

In some cases, the mission power requirement and SOC management requirement are conflicting in nature. For example, if the actual SOC is more than the desired SOC, then the control system must reduce the SOC of the system. This can be done by making the engine-generator system produce less power than the load, which will make the battery system supply the deficit power and thereby maintain the SOC. Therefore, to maintain

SOC, the controller must stop tracking the load and ignore the mission power requirement.

### 3.4 Development of Linear Quadratic Regulator for Hybrid-Electric System

The controller's objective is to meet the electrical load requirement when the battery SOC is at desired SOC level. And when SOC is not at the desired level, the controller should increase or decrease the generator power to maintain the SOC at the desired level.

The Linear Quadratic Regulator (LQR) is a powerful state feedback optimization tool which can be used in a hybrid-electric system to find the optimal gain to stabilize and control a controllable system and achieve the desired characteristics of the system (Nise, 2008). The LQR optimal control algorithm can be applied for hybrid-electric propulsion to split the power demand between the engine/generator and battery pack. These methods have an optimization cost function which can be used to derive optimal control solutions for hybrid-electric systems for Urban Air Mobility (UAM).

Given that the system (A, B) is controllable, then the Linear Quadratic Regulator provides an optimization method which can be used to find the feedback control gains. For the plant model, the primary goal is to minimize the cost function using the control input  $u$ :

$$J = \int_0^{\infty} x(t)' Q x(t) + u(t)' R u(t) dt \quad (48)$$

where  $Q (>0)$  and  $R (>0)$  are positive-definite weighting matrices.

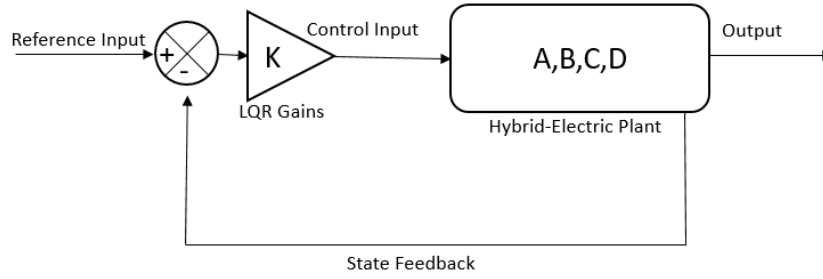


Figure 3.16 LQR Controller

The pictorial representation of the LQR controller with hybrid-electric power plant is shown in Figure (3.32).

### 3.4.1 Augmented State-Space Representation using Integral State

The performance of the LQR controller can be improved by adding an integral state to the system. The integral state of the SOC error has been incorporated in the hybrid-electric system to eliminate the steady state error in SOC. The new state-space model created after adding the integral state is referred to as the augmented state-space model.

The new augmented state-space model is as in Equation (49):

$$\dot{\bar{x}} = \bar{A}\bar{x}(t) + \bar{B}u(t) + \bar{\Gamma}u_d(t) \quad (49)$$

$$\bar{y} = \bar{C}x \quad (50)$$

where:

$$\bar{x} = \begin{bmatrix} \dot{x} \\ \dot{q} \end{bmatrix}, \quad \bar{A} = \begin{bmatrix} A & 0 \\ -C & 0 \end{bmatrix}, \quad \bar{x} = \begin{bmatrix} x \\ q \end{bmatrix}, \quad \bar{B} = \begin{bmatrix} B \\ 0 \end{bmatrix}, \quad \bar{C} = [C \ 0], \quad \bar{\Gamma} = \begin{bmatrix} \Gamma \\ 0 \end{bmatrix}$$

$$\dot{q} = r - y = r - Cx \quad (51)$$

The augmented state-space model in expanded form is

$$\begin{bmatrix} \dot{T} \\ \dot{SOC} \\ \dot{q} \end{bmatrix} = \begin{bmatrix} \frac{-1}{\tau} & 0 & 0 \\ \frac{\alpha_2}{Q_n} & 0 & 0 \\ 0 & -1 & 0 \end{bmatrix} \begin{bmatrix} T \\ SOC \\ q \end{bmatrix} + \begin{bmatrix} \frac{\alpha_1}{\tau} \\ 0 \\ 0 \end{bmatrix} [u^{th}] + \begin{bmatrix} 0 & 0 \\ \frac{-1}{Q_n * v_b(t)} & 0 \\ 0 & 1 \end{bmatrix} \begin{bmatrix} L \\ r \end{bmatrix}$$

$$\begin{bmatrix} T \\ SOC \\ q \end{bmatrix} = \begin{bmatrix} 1 & 0 & 0 \\ 0 & 1 & 0 \\ 0 & 0 & 1 \end{bmatrix} \begin{bmatrix} T \\ SOC \\ q \end{bmatrix}$$

The LQR controller can be considered a system with two parts:

1. Estimating reference/desired states
2. Tuning LQR gains

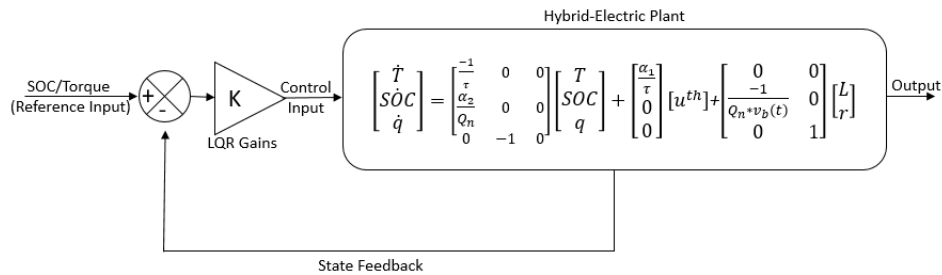


Figure 3.17 LQR controller for Augmented System

The LQR controller with augmented system is shown in Figure (3.33).

### 3.4.2 Estimating Reference/Desired States

The derived augmented state-space model for the hybrid-electric system has three states, namely torque, SOC and integral state. The control design requirement for EFRC's UAM hybrid propulsion system for UAM is most of the electrical power should be generated by the engine/generator system. Therefore, desired torque is the torque the engine should produce to meet the load requirement using the engine/generator system alone. As the electrical load requirement is dynamic in nature, the desired torque can also be dynamic. On the other hand, the desired SOC of the system is generally static and is set according to the type of battery cell used. In general, the desired SOC for most lithium-ion cells is between 80-95%. The chosen desired SOC for modeling and

simulation is 80%. The desired integral SOC error state is zero so that the system reaches a steady state.

### 3.4.3 Tuning LQR Gains

The LQR controller consists of a cost function which is built using the weighting matrices Q and R. These weighting matrices essentially affect the minimization of the cost function and so are the tuning variables. The Q matrix is the weighting matrix for the state of the system. The more weighting given to a state, the more attention will be paid by the controller to track the desired state better. The R matrix is the weighting matrix for the control inputs to the system. The more weighting given to an input, the less input will be used by the controller. The cost function of the LQR controller with Q and R weighting matrices is given in Equation (48).

The tuning of the Q and R matrices can be performed using the Bryson method (Bryson, 2015). In this method, the desired maximum values for the states and controls are chosen. This defines the relative weighting between Q and R, but does not set any hard constraints. The Q matrix can be set as seen in Equation (52).

$$Q = \begin{bmatrix} \frac{1}{(x_{1\max})^2} & 0 & 0 \\ 0 & \frac{1}{(x_{2\max})^2} & 0 \\ 0 & 0 & \frac{1}{(x_{3\max})^2} \end{bmatrix} \quad (52)$$

Similarly, the R matrix can be set as in Equation (53).

$$R = \begin{bmatrix} \frac{1}{(u_{1\max})^2} \end{bmatrix} \quad (53)$$

The Bryson method is followed to find the initial gains of the hybrid electric LQR controller. The initial Q and R matrices for the LQR controller for the hybrid-electric system were set as in Equations (54) and (55):

$$Q = \begin{bmatrix} \frac{1}{(T_{max})^2} & 0 & 0 \\ 0 & \frac{1}{(Soc_{max})^2} & 0 \\ 0 & 0 & \frac{1}{(q_{max})^2} \end{bmatrix} \quad (54)$$

$$R = \left[ \frac{1}{(u_{th\ max})^2} \right] \quad (55)$$

The gains found from the Bryson method were used for initial simulation. To achieve the desired performance, the system was subsequently tuned manually from the initial gains.

### 3.5 Simulation of Hybrid-Electric System

The hybrid-electric system is simulated in MATLAB software using two methods. The hybrid-electric system model of idealized electrical element and state-space model were created in the Simulink and Simscape environment in MATLAB software.

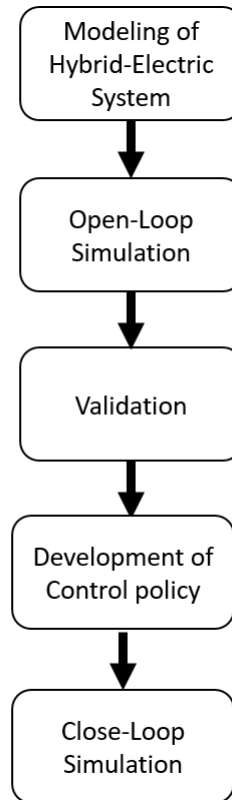


*Figure 3.18* Simulation Workflow

The developed models were used to perform the open-loop simulations, which were then validated with actual experimental results as seen in Figure (3.34). The validated models were then used to develop the control strategy and closed-loop simulations were performed. The simulation models of the open-loop system of the idealized electrical element model and state-space model, along with the closed loop model with LQR controller, are discussed in the following sections.

### **3.5.1 Open-Loop Simulation using Idealized Electrical Element Model**

The Idealized Electrical Element model is simulated using the SIMCAPE electrical elements and Simulink codes as shown in Figure (3.35). The generator, battery and load are modeled as a controlled current source, controller voltage source and variable resistor,

like the free-body diagram of the hybrid-electric system. The model also consists of current and voltage sensors which provide the associated sensor information. The inputs to the system are throttle and load resistance, while outputs are generator current, battery current, load current, bus voltage, and SOC. The load resistance is calculated according to electrical load using the power relation.

Besides the hybrid-electric bus, the model also consists of the following codes:

1. Engine/ Generator Transfer Function
2. SOC Calculator
3. Voltage Calculator

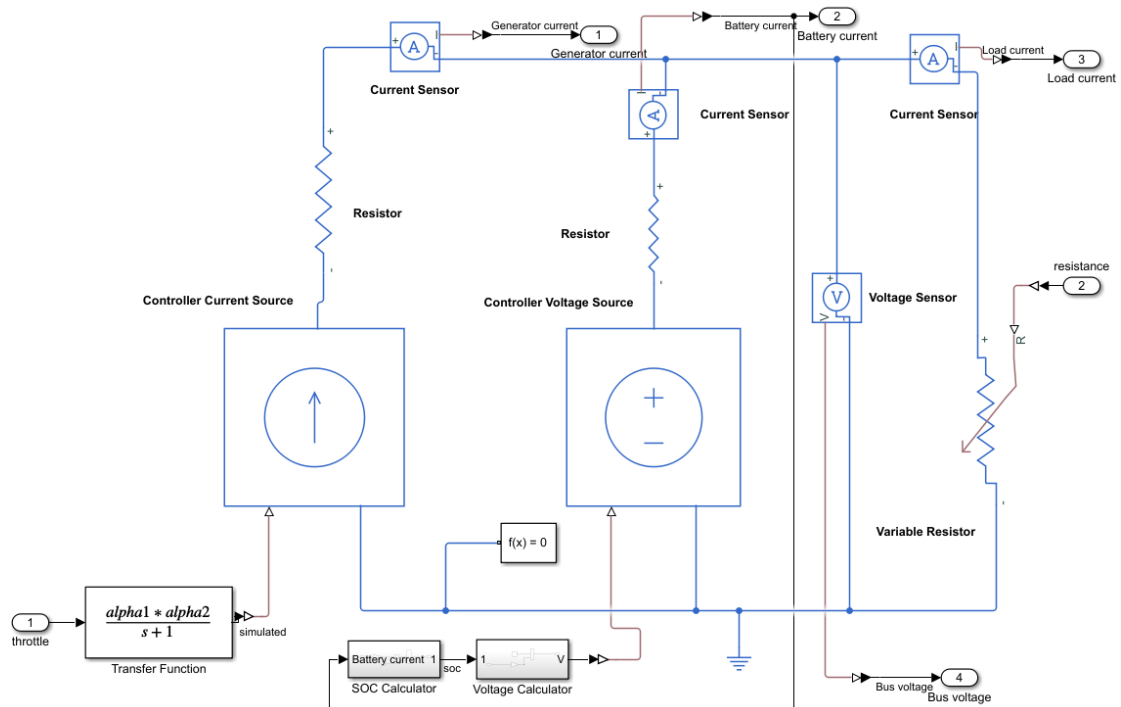


Figure 3.19 Idealized Electrical Element Model

### Engine/Generator Transfer Function

The generator current, which is the input for the hybrid-electric bus, is modeled using a transfer function which consists of the engine constant  $\alpha_1$ , engine time constant  $\tau$  and



generator constant  $\alpha_2$  as the variable. The input to the transfer function is throttle position and output is the generator current.

### SOC Calculator

The SOC calculator consists of the codes seen in Figure (3.36), which are derived using the Coulomb counting equation. The input to the block is battery current, which is obtained from the sensor, while the output is the SOC.

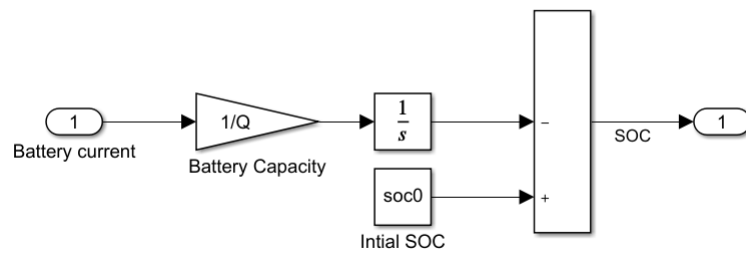


Figure 3.20 SOC Calculator

### Battery Open Circuit Voltage

The battery open circuit voltage block, as seen in Figure (3.37), is used to calculate the battery open circuit voltage which fed into the voltage source of the hybrid-bus model. The input to the block is SOC while the output is the battery open circuit voltage.

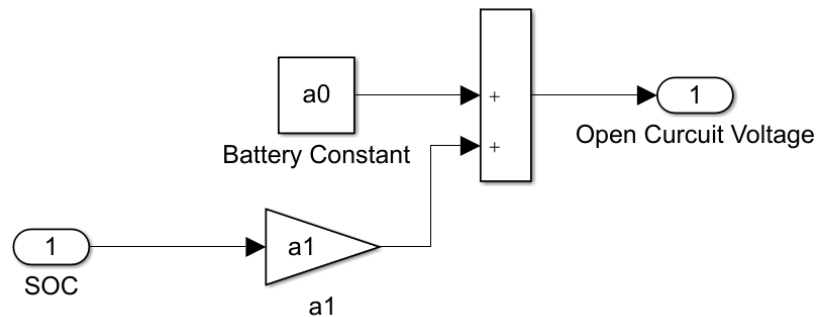


Figure 3.21 Battery Open Circuit Calculator

### 3.5.2 Validation of Idealized Electrical Element Model

The idealized electrical element model is validated using actual experimental results. The hybrid-electric plant which needs to be validated receives the actual experimental throttle and electrical resistance calculated according to the load. The plant model will then generate various system parameters, which are compared with the actual experimental parameters as shown in Figure (3.38)

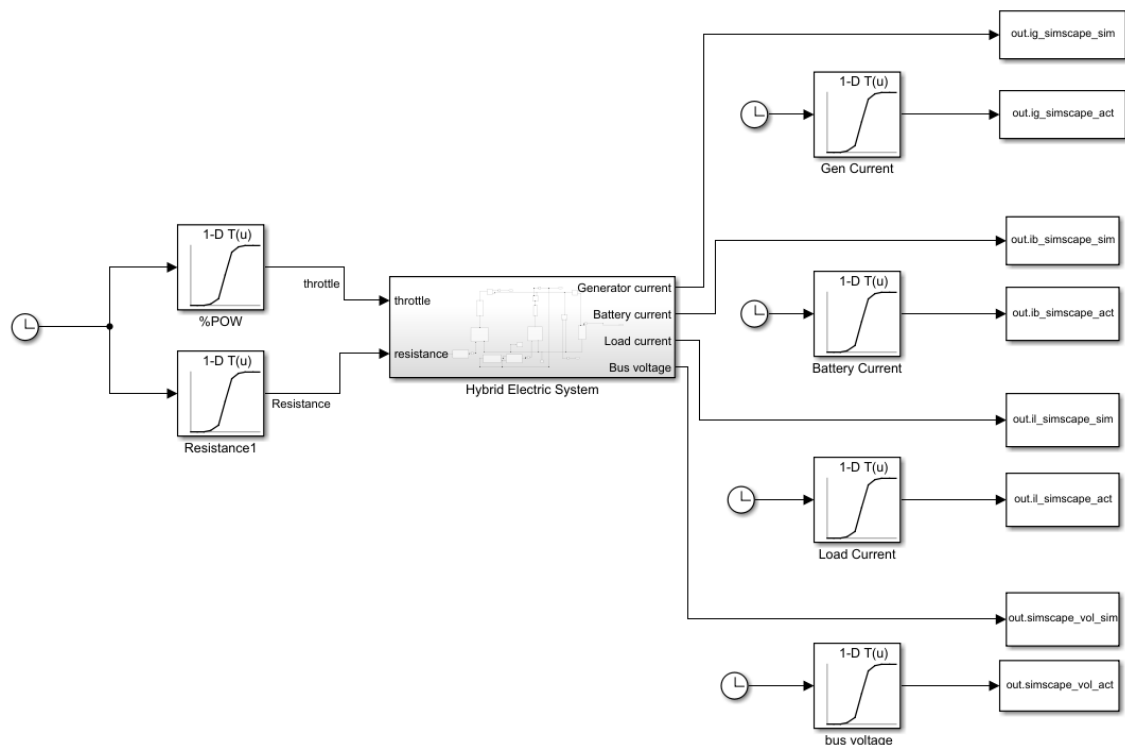


Figure 3.22 Validation of Idealized Electrical Element Model

### 3.5.3 Open-Loop Simulation using State-Space Representation

The open-loop simulation of the state-space representation of the hybrid-electric system is done in Simulink as shown in Figure (3.39). The simulation codes are divided into three parts:

1. Hybrid System

2. Load Current

3. Voltage Calculator

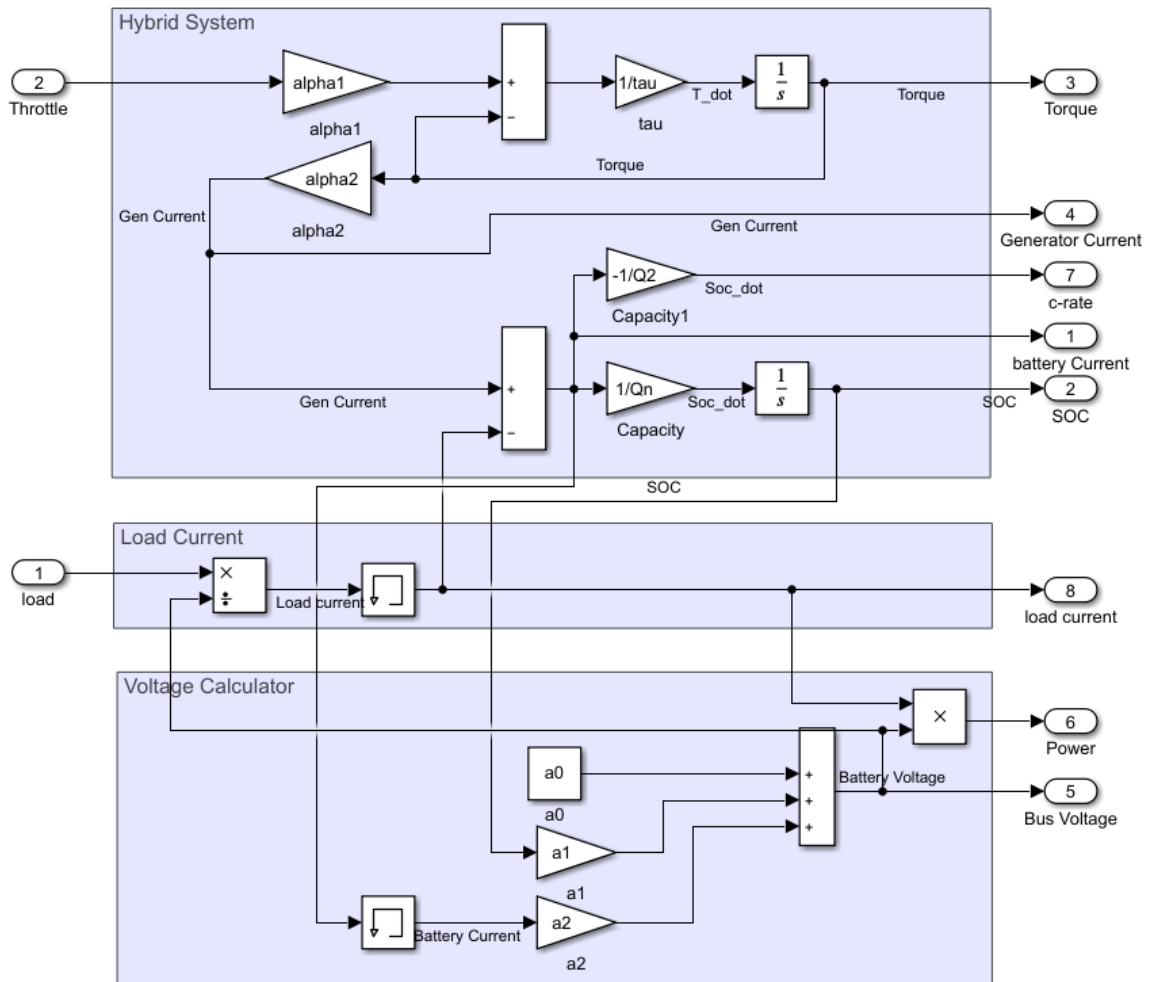


Figure 3.23 State-Space Model of Hybrid Electric System

The hybrid system models the state-space equations, and load current is calculated according to load. The terminal voltage of the batteries is calculated in the voltage calculator.

### 3.5.4 Validation of State-Space Model

The state-space plant model of the hybrid-electric system is validated like the idealized electrical element model. The validation setup consists of the plant model,

which receives the actual experimental load and throttle positions. The output generated by the plant is compared with the actual experimental results as shown in Figure (3.40).

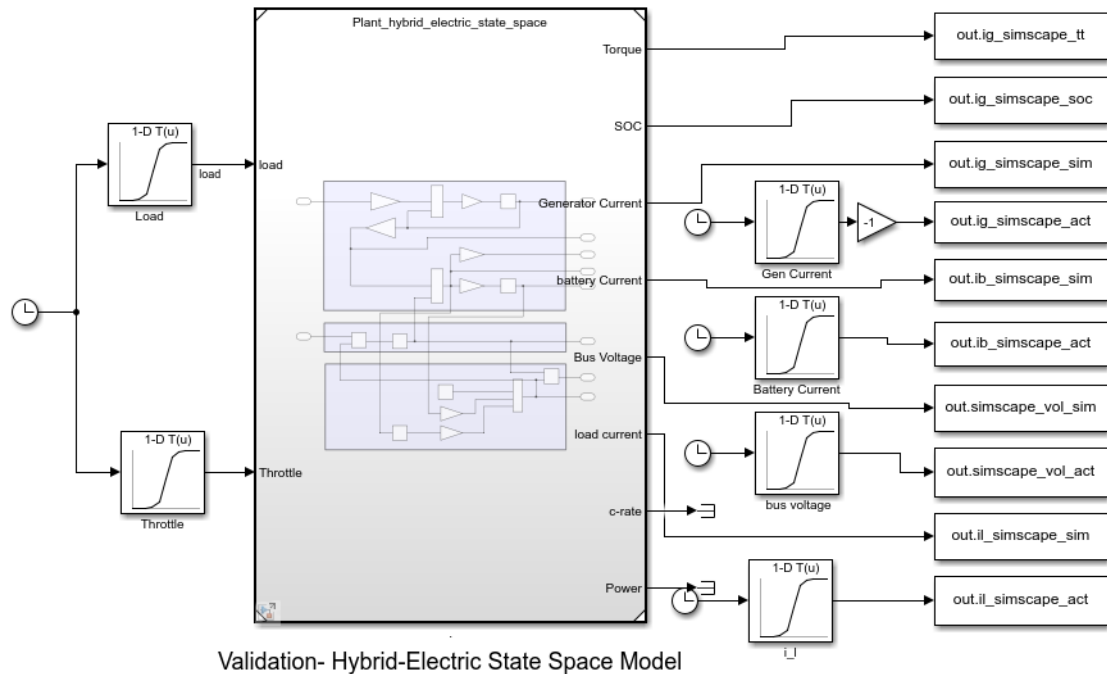


Figure 3.24 Validation of State-Space Model

### 3.5.5 Closed-Loop Simulation using Linear Quadratic Regulator

The closed-loop simulation of the hybrid-electric system is performed using the validated state-space model of the system and LQR controller. The simulation uses the reference blocks to ensure continuity and coherence between the open and closed-loop simulations, as seen in Figure (3.41). The simulation is divided into three blocks:

1. State-Space Hybrid-Electric Plant
2. Reference System
3. LQR Controller

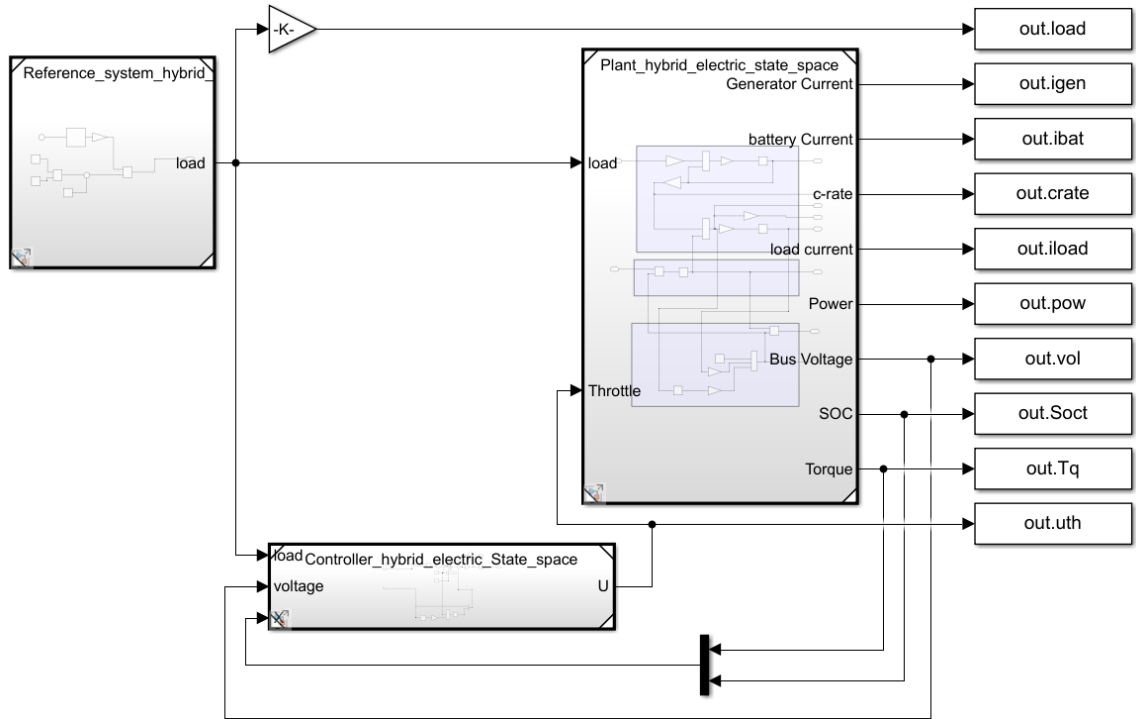


Figure 3.25 Closed-Loop Simulation with LQR Controller

### State-Space Hybrid-Electric Plant

The plant block uses the reference block and consists of the validated state-space model of the hybrid-electric system. The input to the system is engine throttle position and the system generates outputs such as generator current, battery current, battery C-rate, load current, total electrical power, bus voltage, engine torque and SOC while tracking electrical load from the reference system block.

### Reference System

The reference system block generates the electrical load which the system needs to track. The block has no input while the output is the electrical load.

### LQR Controller

The controller block consists of the LQR controller. The LQR controller requires the desired/reference states, which are either defined or calculated according to the system

parameters as shown in Figure (3.42). These desired states are then compared with actual states to find the error, which is finally multiplied with the LQR gain to estimate the optimal control output.

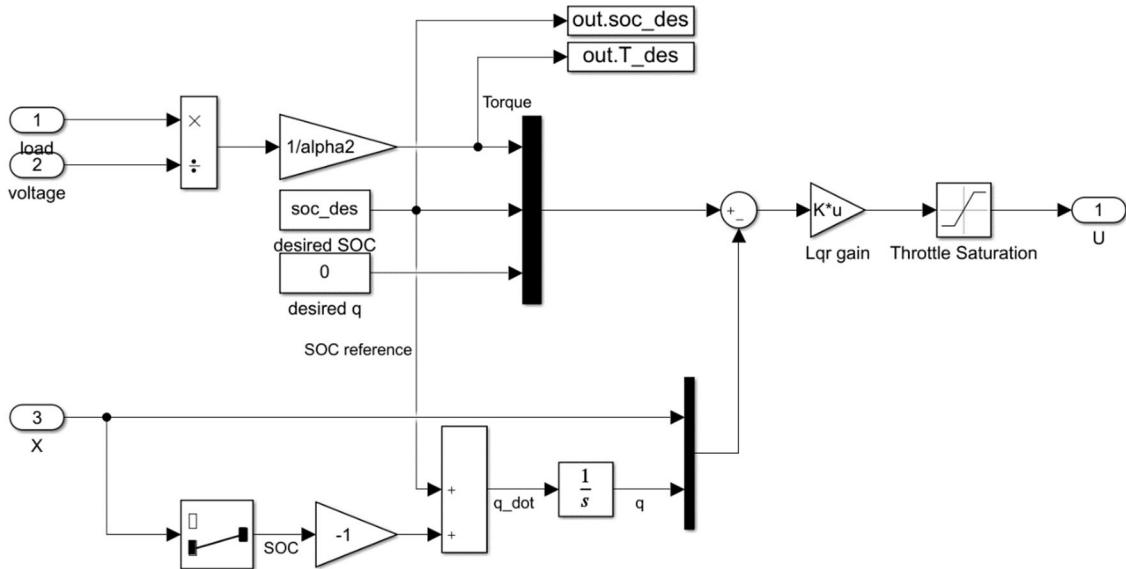
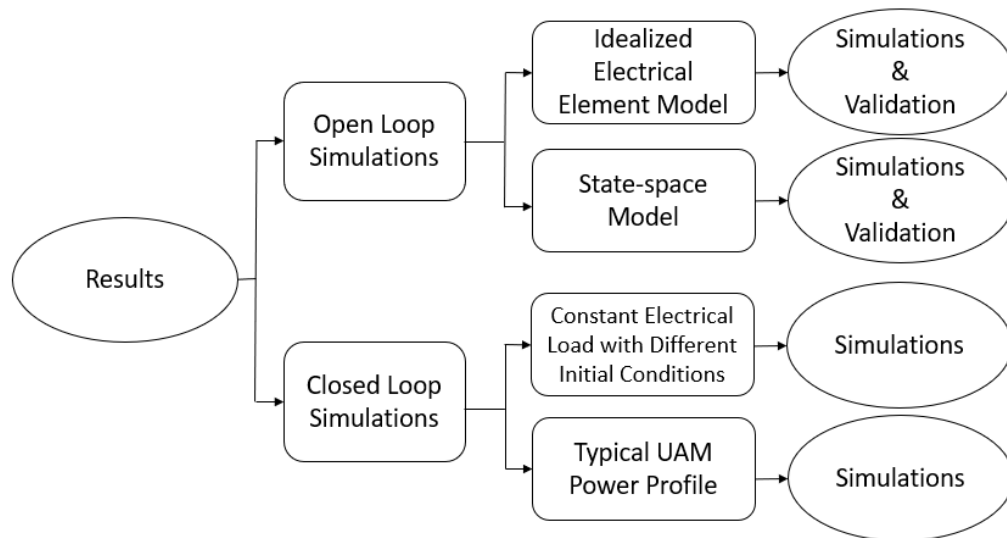


Figure 3.26 LQR Controller for Hybrid-Electric System

The developed LQR controller, as well as the actual codes of the different models, are discussed in this chapter. The hybrid-electric system is modeled as the idealized electrical element and governing equations have been found to represent the system as a state-space model in this chapter. The results of the simulation models are presented in next the chapter.

## 4. Results

Results from open-loop and closed-loop simulations are presented in this chapter. The open-loop simulation consists of results from idealized electrical element model and state-space model. The simulation and validation results of both the models are shown. The closed-loop simulation consists of the results from the hybrid-electric state-space plant with LQR controller, as seen in Figure (4.43). The closed-loop system was simulated under constant electrical load with different initial conditions as well as with a typical UAM power profile.



*Figure 4.27* Overview of Results from Different Simulation Models

### 4.1. Results of Open-Loop Idealized Electrical Element Model

Open-loop simulation results from idealized electrical element models are shown in this section. The important parameters of a hybrid-electric system are generator current, battery current, bus voltage and load current. Therefore, the simulation and experimental results of these parameters are shown.

### 4.1.1 Generator Current Validation

The simulation results of the generator current from the idealized electrical element model were validated with the experimental results in Figure (4.44). The figure consists of the simulation and experimental results on the top and residual error on the bottom. The simulation results tend to follow the experimental results with error mostly between -15% to 5%.

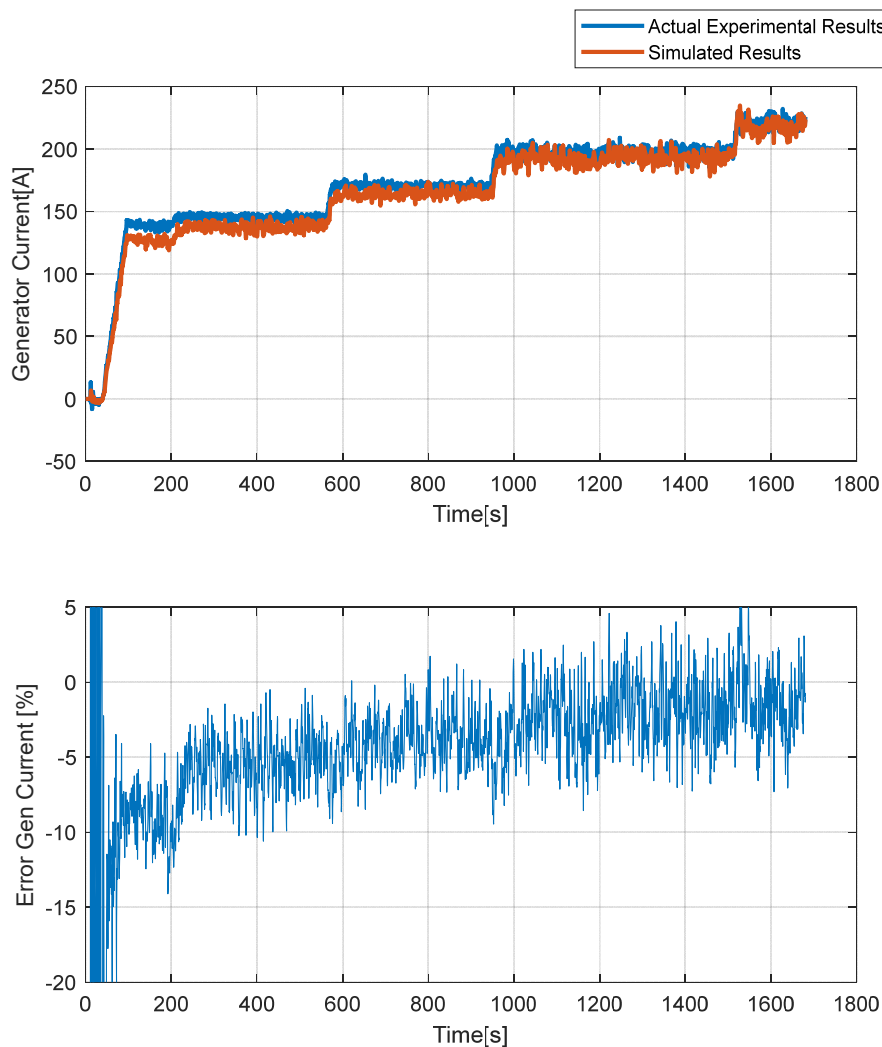


Figure 4.28 Idealized Electrical Element Model: Generator Current Validation



### 4.1.2 Battery Current Validation

The result of battery current validation of the idealized electrical element model is shown in Figure (4.45). The simulation and experimental results of battery current are shown on the top of Figure (4.45) whereas the error plot is shown at the bottom. The simulation results seem to follow the first-order dynamics of the experimental results.

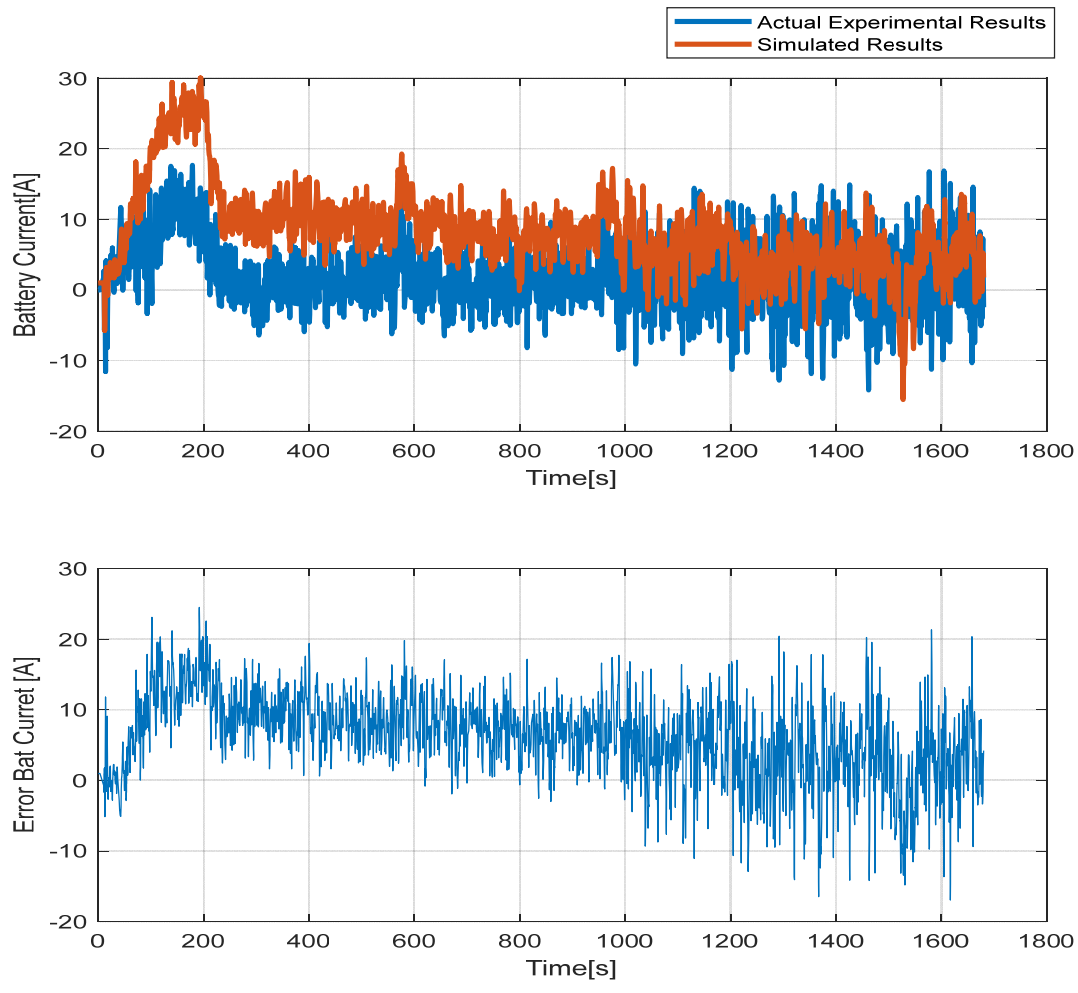


Figure 4.29 Idealized Electrical Element Model; Battery Current Validation

### 4.1.3 Hybrid- Electric Bus Voltage Validation

The simulation and experimental results of hybrid-electric bus voltage of the idealized electrical model are shown in Figure (4.46). Like the battery current validation, the simulated bus voltage captures the first-order dynamics of the experimental results with some error.

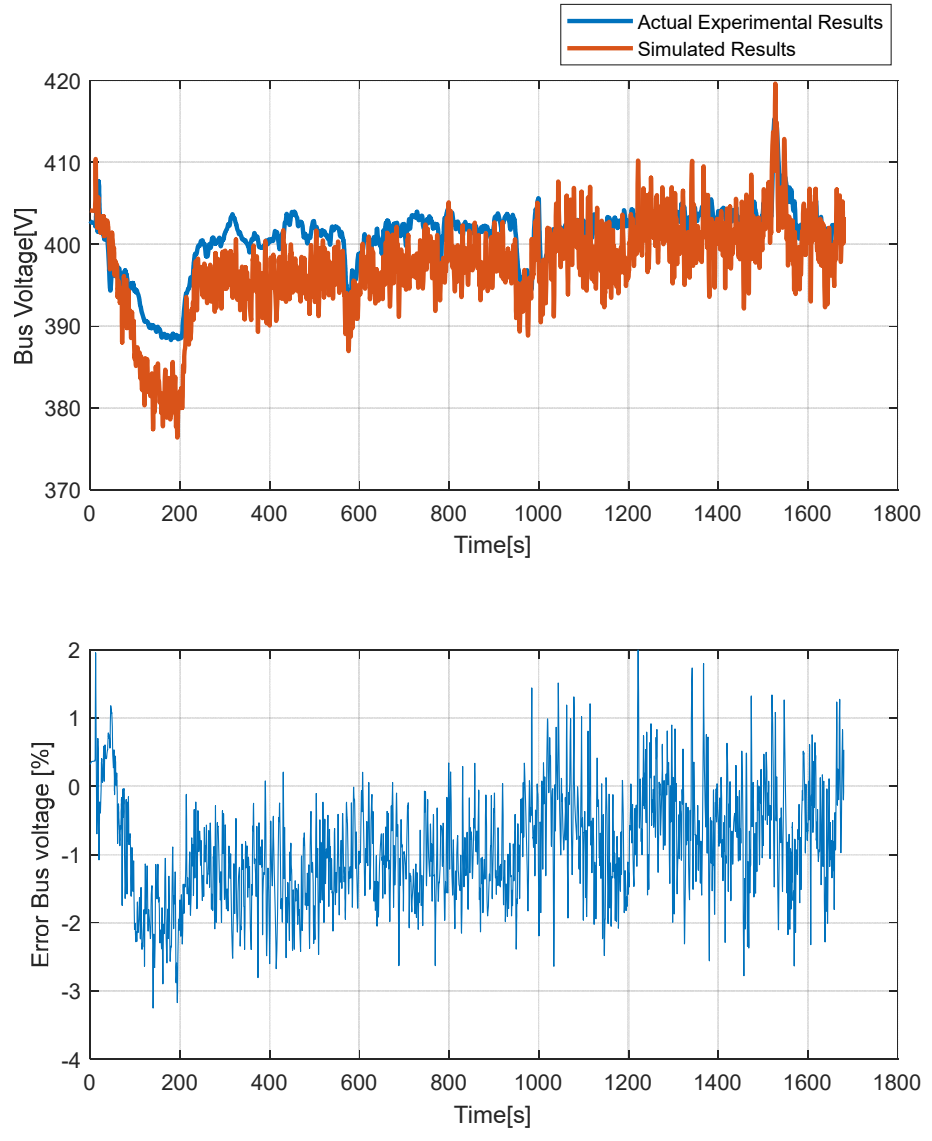


Figure 4.30 Idealized Electrical Element Model: Bus Voltage Validation

### 4.1.4 Electrical Load Current Validation

The electrical load current simulation and validation are shown in Figure (4.47). The graph consist of validation and error plots. The simulation and experimental results tends to be in agreement with each other.

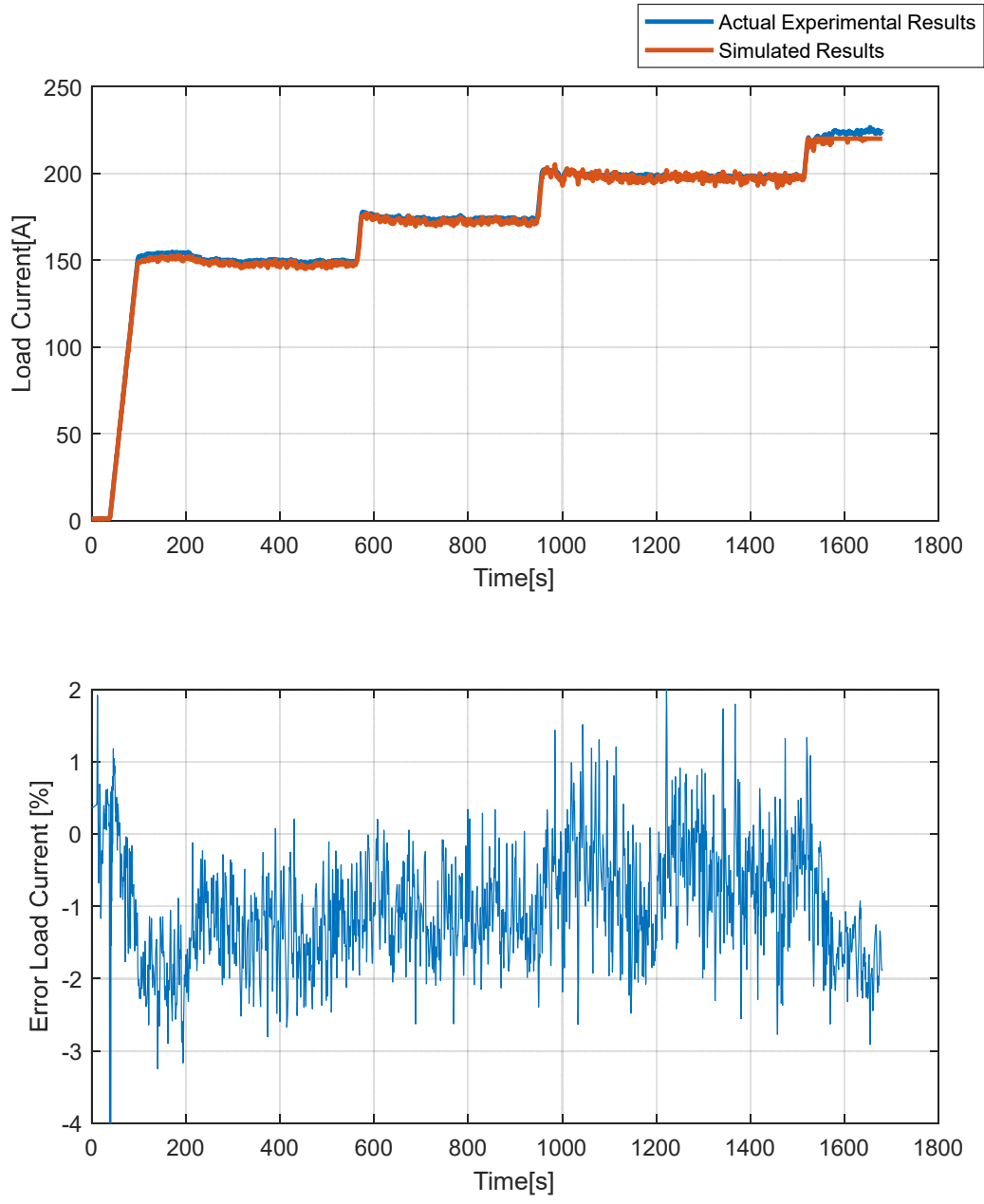


Figure 4.31 Idealized Electrical Element Model: Load Current Validation

## 4.2 Results of Open-Loop State-Space Model

The simulation results of the open-loop state-space model are discussed in these sections. Like the idealized electrical element model validation, simulation results of generator current, battery current, bus voltage and load current are presented and validated here.

### 4.2.1 Generator Current Validation

The simulated values of generator current obtained from the state-space model of the hybrid electric system are compared against the experimental results along with the residual error plot. The generator current simulated using the state-space model seems to follow the trend of the experimental results with some error, as shown in Figure (4.48).

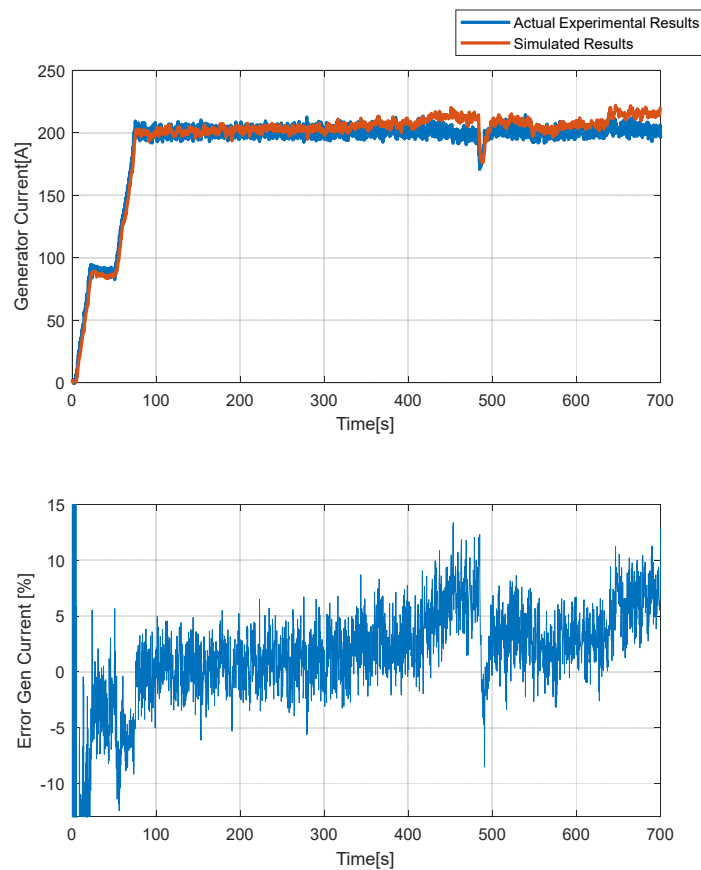


Figure 4.32 State Space Model: Generator Current Validation

## 4.2.2 Hybrid-Electric Bus Voltage Validation

The validation plot of the hybrid-electric bus voltage is shown in Figure (4.49). The simulated voltage seems to follow the experimental results with error between -6% to 2%.

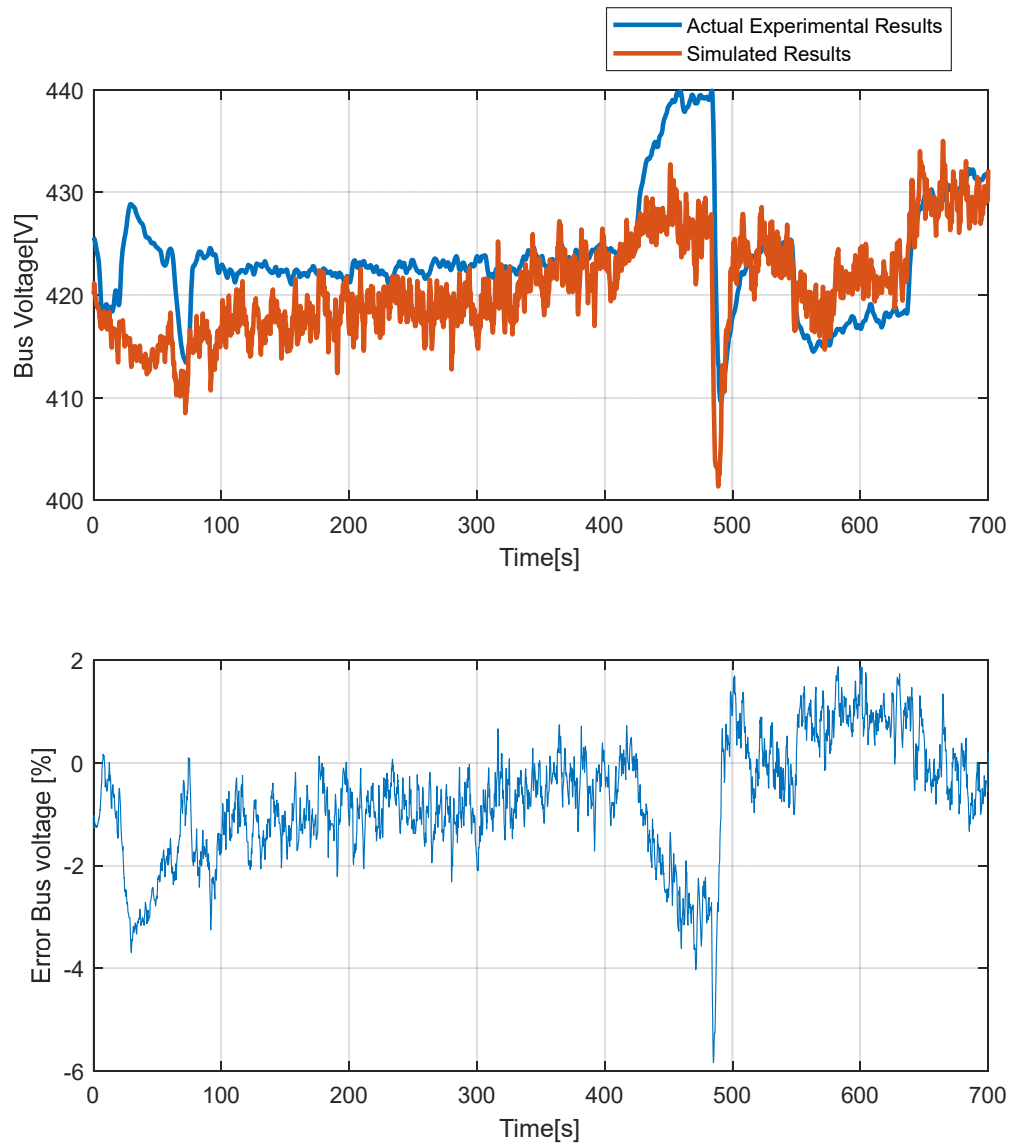


Figure 4.33 State-Space Model: Bus Voltage Validation

### 4.2.3 Hybrid-Electric Battery Current Validation

The validation plot of battery current with the error plot from the state-space model are presented in Figure (4.50). The error between the actual battery current and the simulated battery current is generally between -10A to 20A.

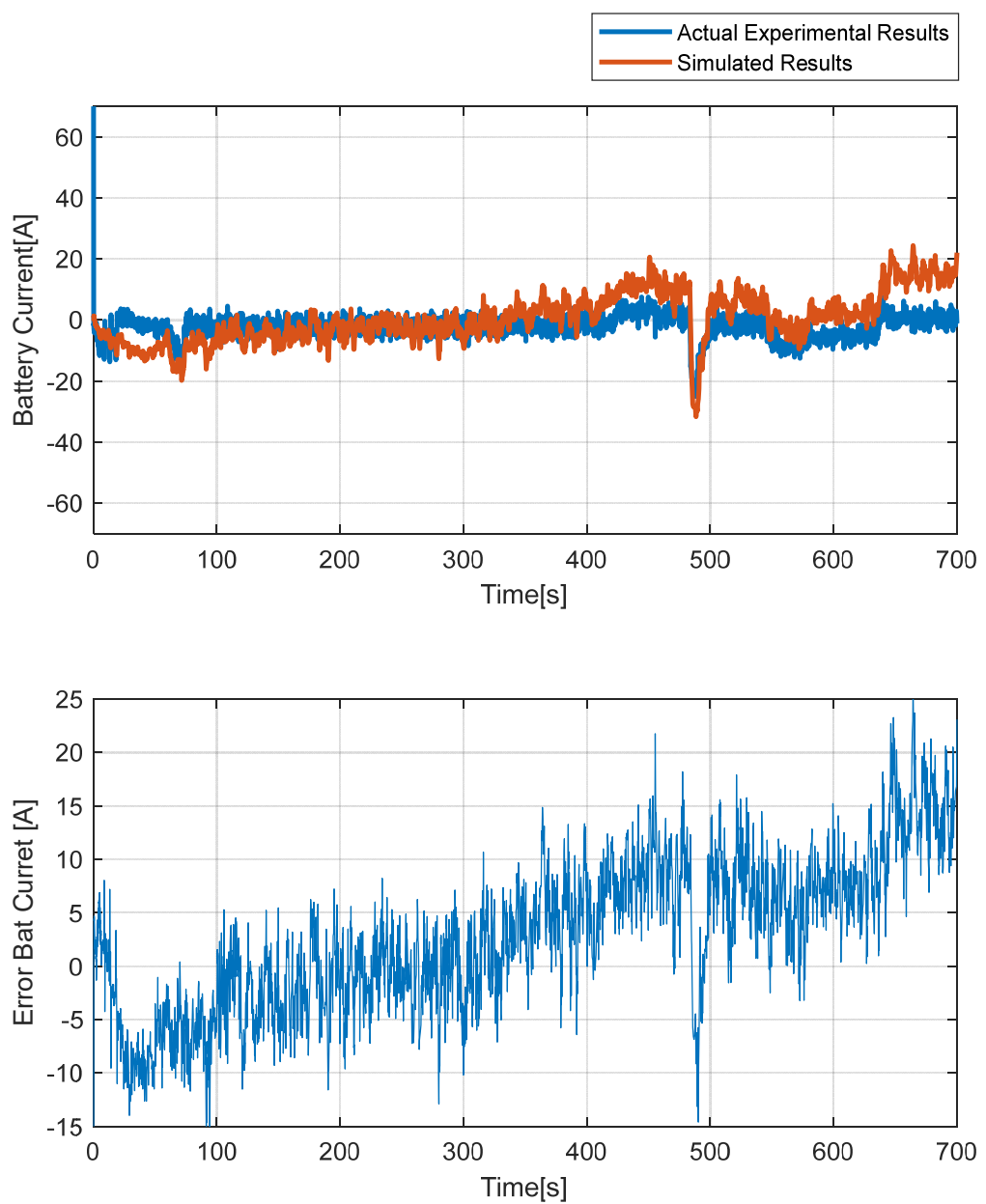


Figure 4.34 State Space Model: Battery Current Validation

#### 4.2.4 Electrical Load Current Validation

The validation plot of the load current is shown in Figure (4.51). The simulated results are mostly in agreement with the experimental results.

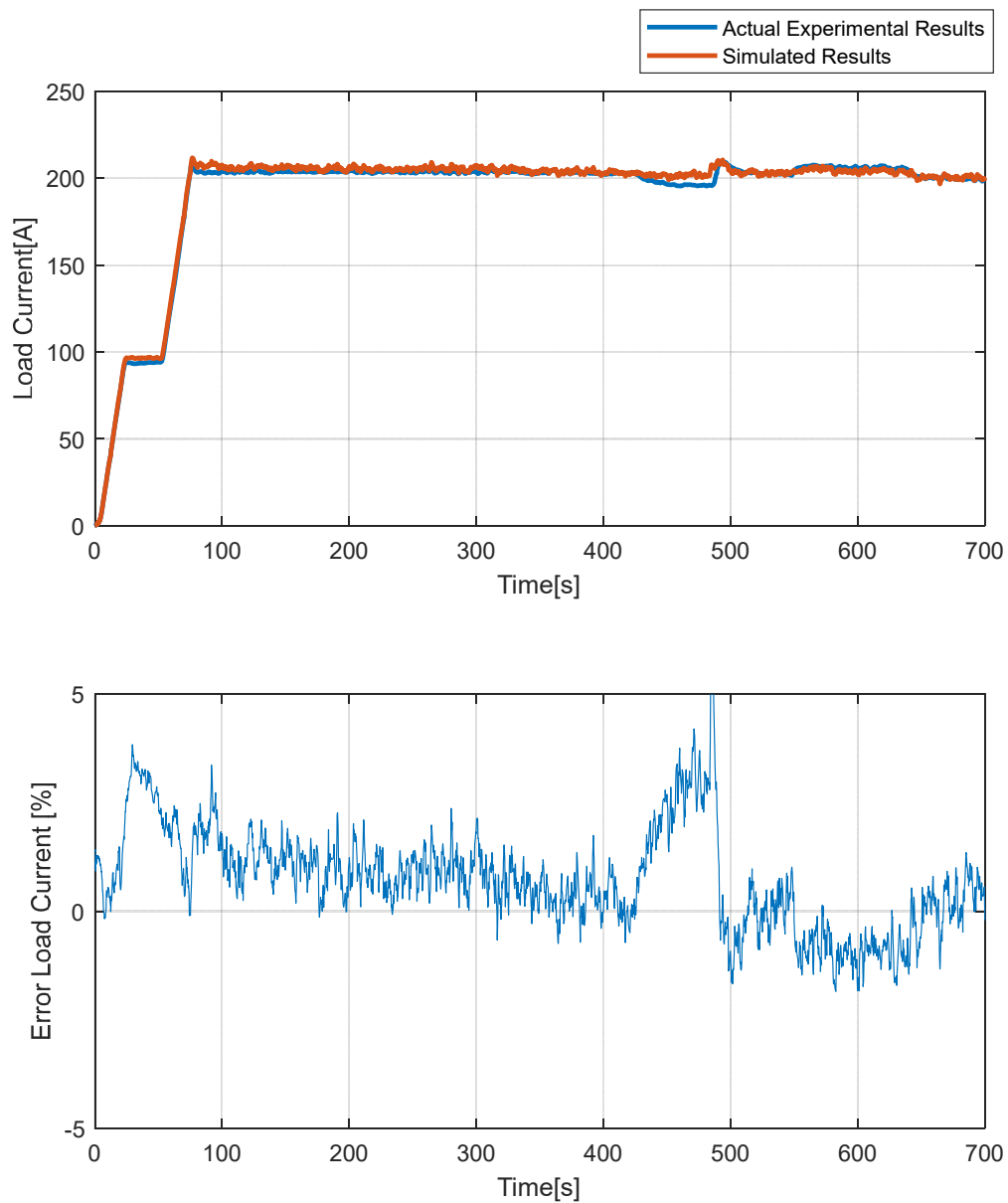


Figure 4.35 State-Space Model Validation: Load Current

### **4.3 Results of Closed-Loop Model with Linear Quadratic Regulator**

The closed-loop system with hybrid-electric state-space plant and LQR controller is simulated. The performance of the controller was evaluated under constant load and a typical UAM aircraft power profile.

#### **4.3.1 Performance of the Controller under Constant Electrical Load**

A constant electrical load of 60 kW was applied to the hybrid-electric model to simulate the closed-loop system response and evaluate the controller performance. The initial SOC of the battery system is set at 85%, which is more than the desired SOC of 80%. The response of the system is presented in Figure (4.52). The figure consists of a plot showing electrical load and total combined power produced by the system on the top, while power obtained from the generator and battery are shown in the middle and bottom plots respectively. It was found from the simulation results that the controller was able to maintain the SOC of the battery at the desired level by commanding the engine /generator system to produce less electrical power than the required electrical load. Once the desired SOC level is reached, the controller commands the engine/generator system to produce power according to the required electrical load, thereby reaching the steady state.



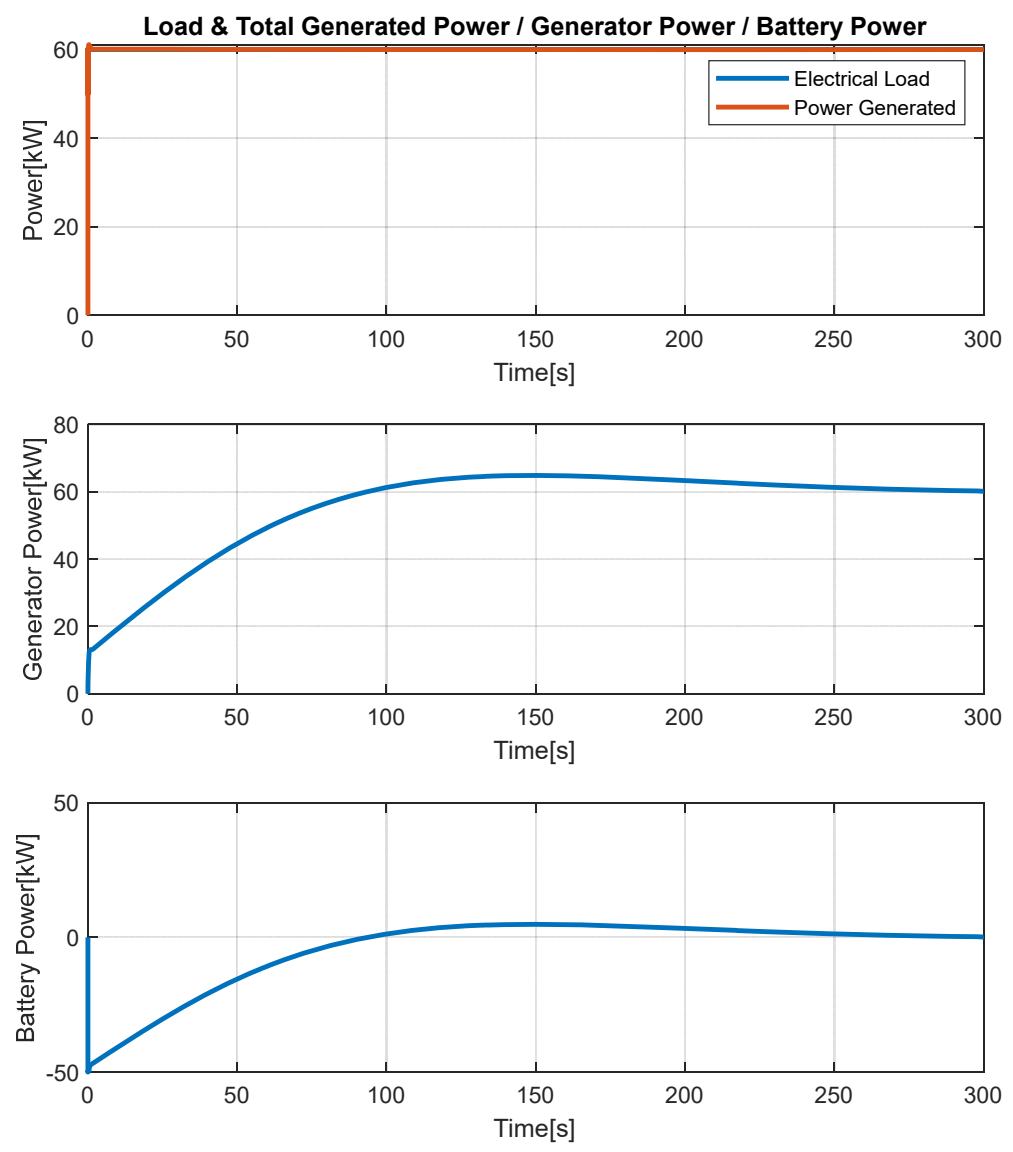


Figure 4.36 Closed-Loop System performance under Constant Load

### 4.3.2 System States and other Critical Parameters under Constant Load

The system states and other critical parameters under constant electrical load are shown in Figure (4.53). The plot of desired and actual torque along with desired and actual SOC plots are positioned on the top, while the c-rate, bus voltage and throttle position are shown on the bottom. The figure demonstrates that the controller was able to track desired torque and desired SOC.

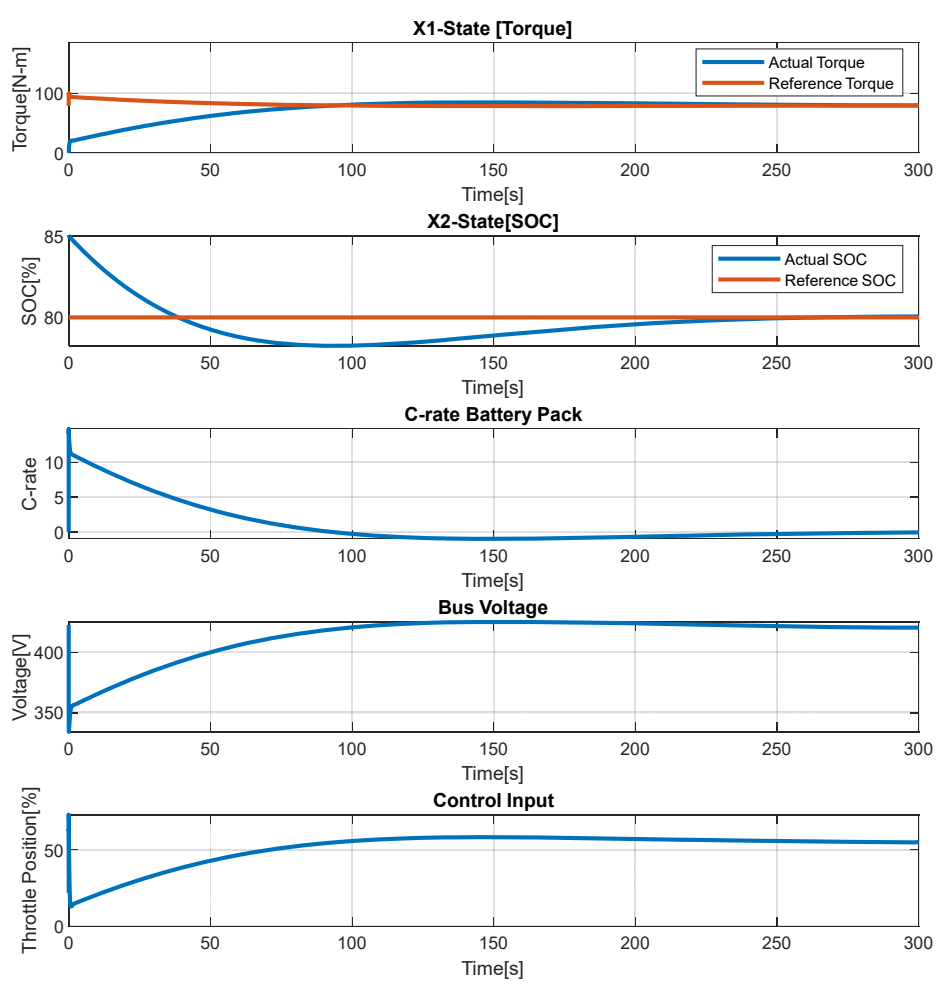


Figure 4.37 System States and other Critical Parameters under Constant Load

### 4.3.3 Phase-Plane Trajectories of the System under Constant Load and Different Initial Conditions

A phase-plane plot of the system was created under a constant load and different initial torque and SOC. It can be observed from the simulation results in Figure (4.54) that, irrespective of initial conditions, all the trajectories reach the same focal point. Therefore, the controller is able achieve the desired steady state for a wide range of initial conditions.

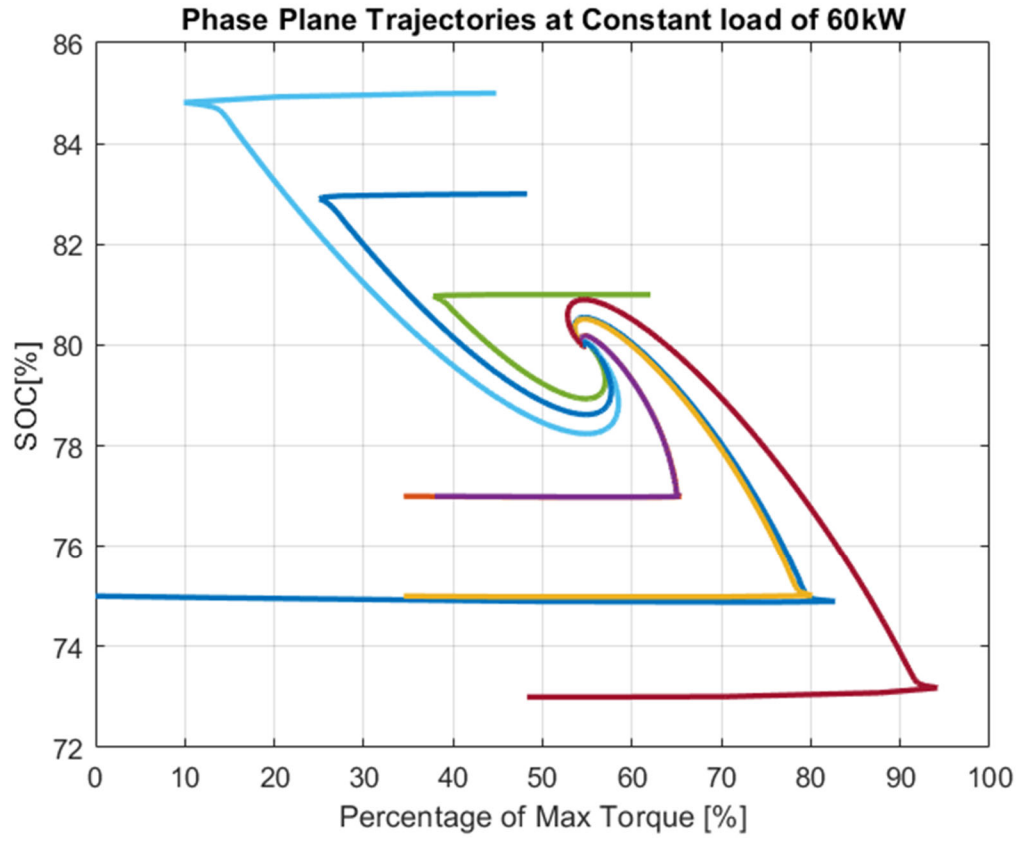


Figure 4.38 Phase-Plane Trajectories of the System

### 4.3.4 Performance of the Controller under Typical UAM Power Profile

The performance of the controller was also evaluated in a typical UAM aircraft mission profile. It can be seen from Figure (4.55) that the controller was able to meet the mission requirements of UAM aircraft.

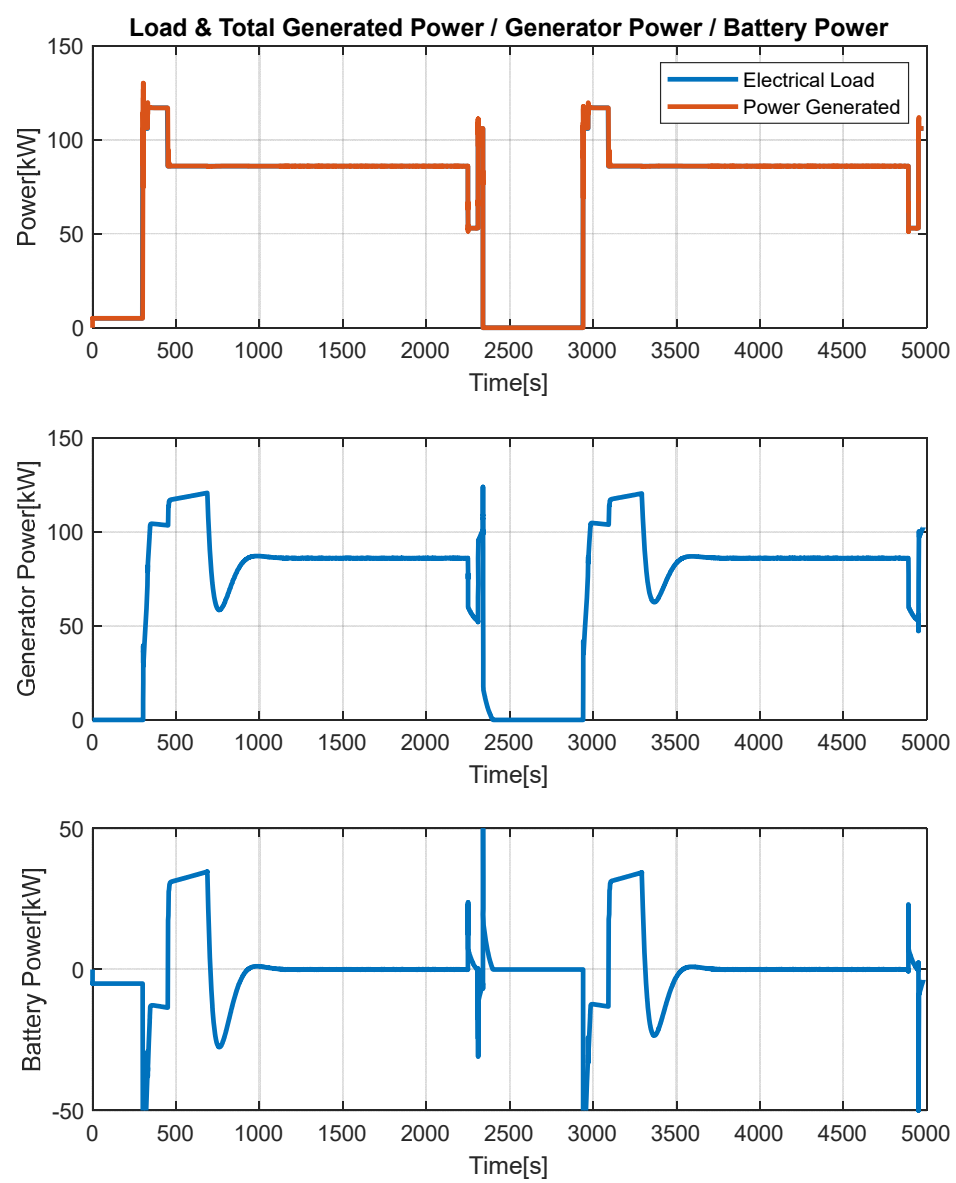


Figure 4.39 Performance of the Controller under Typical UAM Power Profile

### 4.3.5 System States and Other Parameters under Typical UAM Power Profile

The simulation results of different states and other parameters under a typical UAM power profile are shown in Figure (4.56). It can be observed that the controller was able to track the desired states while meeting the mission requirements.

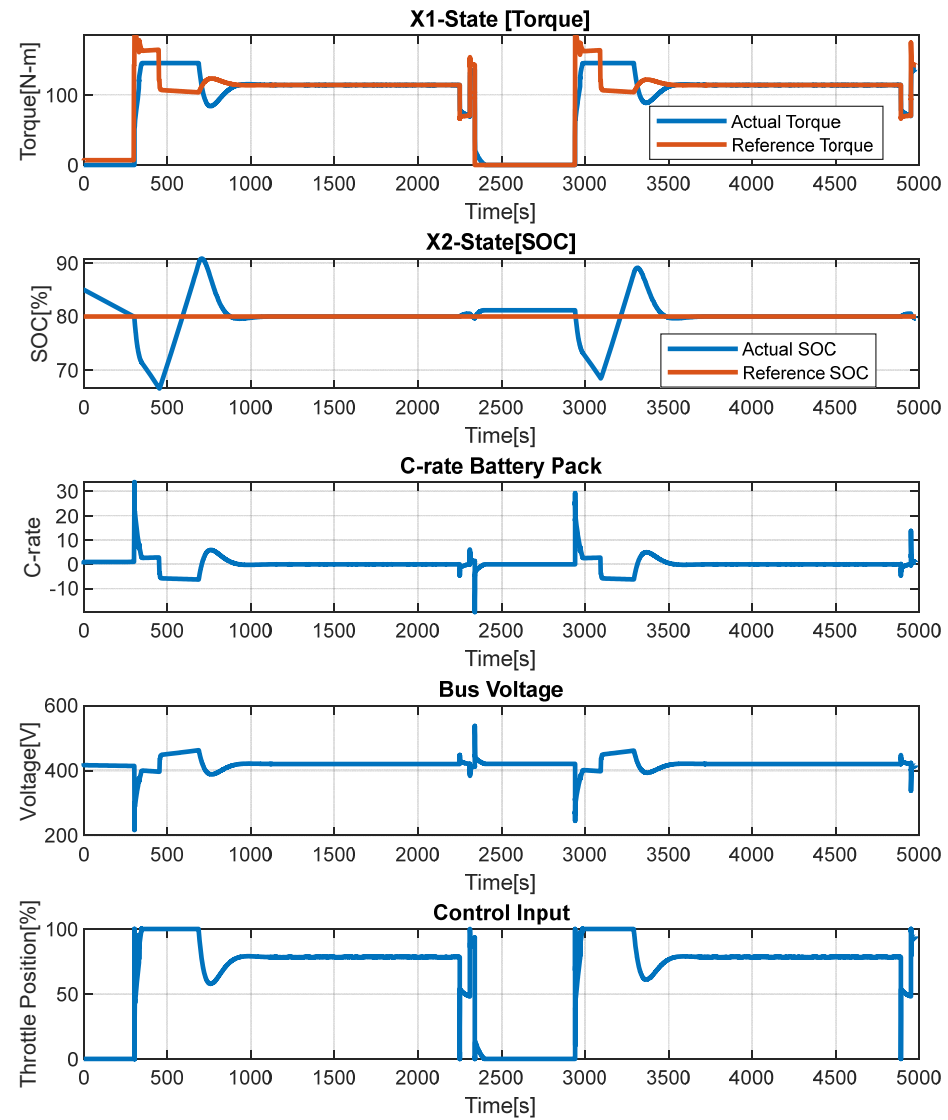


Figure 4.40 System States and Other Parameters under Typical UAM Power Profile

## **5. Discussions, Recommendation and Conclusion**

The primary objective of modeling, simulation and validation of the Hybrid-Electric system has been done using the Idealized Electrical Element and the state-space model of the system. The developed models were able to capture the first-order dynamics of the hybrid-electric system with some error. The validated models can be helpful in developing control algorithms as well as testing and integration of hardware and software of the hybrid-electric system and subsystems.

Control laws were also successfully developed to meet the mission requirements of the hybrid-electric system. Another objective of the thesis was completed by developing the LQR controller. The developed LQR controller was able to track the desired state without steady state error.

### **5.1. Modeling of Hybrid-Electric System**

The developed models are found to capture the first-order dynamics of various system and sub-system parameters. However, there are some advantages and disadvantages with both the idealized electrical model and the state-space model.

The idealized electrical element model is simple and can be easily used to model the hybrid-electric system. Using this method, the system performance can be improved by modifying/adding different idealized components without increasing complexity. For example, the battery is modeled as a combination of a voltage source and resistance. The configuration of the battery can be easily modified by adding a series of resistors and capacitors to capture the higher-order dynamics. The addition of these components might improve the system performance without adding complexity.

The idealized element method is not amenable to the application of modern control methods. Modern control is helpful in analyzing and developing the control systems. Further study is recommended on the idealized element methods to capture the higher-order dynamics with improved performance, which can facilitate the development of the control policies.

On the other hand, the concepts of modern control theory can be easily applied to the state-space model of the hybrid-electric system. This helps in the analysis and design of control logic. The existing control policies and methods, like full state feedback control, output feedback control, optimal control, and adaptive control, can be easily applied to the state-space model.

As state-space representations are based on a linearized system model, it might be difficult to capture some of the non-linear behavior using the linearized model. Unlike the idealized element model, modification of the existing system might be difficult to improve the system performance. Additionally, throughout the modeling, the speed of the shaft was assumed to be constant. There may be hybrid-electric systems where the speed of the shaft is changing enough to not be considered as constant. Therefore, further study is recommended to improve the performance of the model along with wider applications.

## **5.2 Linear Quadratic Controller for Hybrid-Electric System**

The LQR for the hybrid-electric system is found to be helpful for the development and implementation of the optimal control solution for the hybrid-electric system. The energy management between the engine/generator and battery is successfully balanced to meet the different mission requirements. The performance of the system can be changed and tuned to achieve the requirements by changing the gains of the required weighting

matrices. The application of an LQR controller can further be useful for the hybrid-electric system where the speed of the shaft is not constant and is controlled by an additional control input to the generator. The LQR control can not only be used for weighting the different states but also the weighting the different control inputs to the hybrid-electric system. Therefore, further study is recommended to expand the scope of usage of the LQR controller to different hybrid-electric systems.

### **5.3 Bus Voltage as Control Parameter**

The controls requirement of the hybrid-electric system was derived by tracking engine torque using electrical load and tracking the SOC. The bus voltage of the hybrid electric system is sensitive to changes in the electric load and battery characteristics. Thus, bus voltage can also be used in tracking system performance and as a controls parameter. Therefore, further study is recommended to identify different system parameters which can be used to track the system better in order to meet the mission requirements of the system.



## REFERENCES

- Bellman, R. (1957). *Dynamic Programming*. Princeton, NJ, USA: Princeton Univ. Press.
- Bertsekas, D.P. (2007). *Dynamic Programming and Optimal Control*,. 4th ed. A: . Belmont, MA, USA: Athena Scientific.
- Brogan, W. L. (1991). *Modern Control Theory*. Prentice-Hall.
- Bryson, A.E. (2015). *Control of Spacecraft and Aircraft*. Princeton, NJ: Princeton University Press.
- Collins, K. C., Anderson, R., Currier, P., Fernandes, R., Lahaji, S., and Shivakumar, J. (2021). Analysis of Bus Voltage Sag during High Battery Power Operations on Hybrid Electric Urban Air Mobility Vehicles. *77th Annual Forum & Technology Display, May 10-14, 2021*. Vertical Flight Society.
- Collins, K., Currier, P., Prazenica, R., and Anderson, R. (2021). Real-time Load Following with a 100kW Hybrid-Electric Generator System of an eVTOL Power Profile Simulation in a Turbulent Atmosphere. *Vertical Flight Society*. Vertical Flight Society.
- Crabtree, E. K. (2015). The Energy-Storage Frontier: Lithium-Ion Batteries and Beyond. *MRS Bulletin*, Cambridge University Press, Vol. 40, No. 12, pp. 1067-1078.
- dSPACE. (2021). *MicroAutoBox II*. Retrieved from dSPACE:  
<https://www.dspace.com/en/inc/home/products/hw/micautob/microautobox2.cfm>.
- FAA. (2020, October 08). *Urban Air Mobility and Advanced Air Mobility*. Retrieved from FAA: [https://www.faa.gov/uas/advanced\\_operations/urban\\_air\\_mobility/](https://www.faa.gov/uas/advanced_operations/urban_air_mobility/).

- Finger, D. F., Braun, C., and Bil, C. (2020). Comparative Assessment of Parallel-Hybrid-Electric Propulsion Systems for Four Different Aircraft. *Journal of Aircraft*, 57(5), 843-853.
- Gao, J. P., Zhu, G.-M., and Strangas G. E. (2009). Equivalent Fuel Consumption Optimal Control of a Series Hybrid Electric Vehicle. *Proc. Inst. Mech. Eng., Part D: J. Autom. Eng.*, Vol. 223, No. 8, 1003–1018.
- Goyal, R. R. (2018). *Urban air mobility (UAM) market study*. NASA.
- Huria, T. E., Ceraolo, M., Gazzarri, J., and Jackey, R. (2012). High Fidelity Electrical Model with Thermal Dependence for Characterization and Simulation of High Power Lithium Battery Cells. *IEEE International Electric Vehicle Conference*. pp. 1-8.
- Jensen, H. K. (2020). *Samsung INR18650-20S 2000mAh (Cyan)*. Retrieved from Lygte: [https://lygte-info.dk/review/batteries2012/Samsung%20INR18650-20S%202000mAh%20\(Cyan\)%20UK.html](https://lygte-info.dk/review/batteries2012/Samsung%20INR18650-20S%202000mAh%20(Cyan)%20UK.html).
- Jalil, N., Kheir, N. A., and Salman, M. (1997). A Rule-Based Energy Management Strategy for a Series Hybrid Vehicle. *Proceedings of the 1997 American Control Conference*, Vol. 1, pp. 689–693.
- Joby, A. (n.d.). *Home*. Retrieved from Joby: <https://www.jobyaviation.com/>.
- Johnson, W. C. (2019). *UAM Coordination and Assessment Team (UCAT)*. NASA UAM for ENRI Technical Interchange Meeting.
- Kim, H. D. (2010). Distributed Propulsion Vehicles. *27th International Congress of the Aeronautical Sciences*.

- Kim, H. D., Perry, A., and Ansell, P. (2018). A Review of Distributed Electric Propulsion Concepts for Air Vehicle Technology. *AIAA/IEEE Electric Aircraft Technologies Symposium*, AIAA 2018-4998.
- Lahaji, S. A., Anderson, R., Currier, P., and Collins, K. (2021). Modeling of a Hybrid-Electric System and Design of Load-Following Control Law on Hybrid-Electric Urban Air Mobility Power Plants. *Forum 77*. Vertical Flight Society.
- Lilly, J. (2017). *Aviation Propulsive Lithium-Ion Battery Packs State-of-Charge and State-of-Health Estimations and Propulsive Battery System Weight Analysis*. Embry-Riddle Aeronautical University Master's Thesis.
- Lin, C.-C., Peng, H., Grizzle, J. W., and Kang, J.-M. (2003). Power Management Strategy for a Parallel Hybrid Electric Truck. *IEEE Transactions on Control Systems Technology*, Vol. 11, No. 6, pp. 839-849.
- Malikopoulos, A. A. (2014). Supervisory Power Management Control Algorithms for Hybrid Electric Vehicles: A Survey. *IEEE Transactions on Intelligent Transportation Systems*, Vol. 15, No. 5, pp. 1869-1885.
- Malkapure, H. G. and Chidambaram, M. (2014). Comparison of Two Methods of Incorporating an Integral Action in Linear Quadratic Regulator. *IFAC Proceedings Volumes*, Vol. 47, No. 1, pp. 55-61.
- NASA. (n.d.). *Advanced Air Mobility*. Retrieved from AAM: <https://www.nasa.gov/Aam>
- Ng, S., Moo, C.-S., Chen, Y.-P., and Hsieh, Y. C. (2009). Enhanced Coulomb Counting Method for Estimating State-of-Charge and State-of-Health of Lithium-Ion Batteries, *Applied Energy*, Vol. 86, No. 9, pp. 1506-1511.
- Nise., N. S. (2008). *Control Systems Engineering*. John Wiley & Sons, Inc.

- Putra, W. S., Dewangga, P. R., Cahyadi, A., and Wahyunggoro, O. (2015). Current Estimation using Thevenin Battery Model. *Electric Vehicular Technology and Industrial, Mechanical, Electrical and Chemical Engineering*, pp. 5-9.
- Ripaccioli, G., Bernardini, Di Cairano, S., Bemporad, A., and Kolmanovsky, I. V. (2010). A Stochastic Model Predictive Control Approach for Series Hybrid Electric Vehicle Power Management. *Proceedings of the 2010 American Control Conference*, 2010, pp. 5844-5849
- Ross, D. K. (2006). Hydrogen Storage: The Major Technological Barrier to the Development of Hydrogen Fuel Cell Cars, *Vacuum*, Vol. 80, No. 10, pp. 1084-1089.
- Rotax, A. E. (2021). *Rotax 915 is* . Retrieved from iSC. Rotax 915 iS / iSC : <https://www.flyrotax.com/produkte/detail/rotax-915-is-isc.html>
- Samsung20s. (2021). *Samsung 20s 18650 2000mAh 30A battery*. Retrieved from INR18650-20S. 18650BatteryStore.com.: <https://www.18650batterystore.com/products/samsung-20s>.
- Trajković, L. (2005). Nonlinear Circuits, *The Electrical Engineering Handbook* (Ed: Wai-Kai Chen),. Academic Press, pp.75–77.
- VerdeGo. (2021). *about*. Retrieved from verdegoaero: <https://www.verdegoaero.com/>.
- Wang, Z., Li, W., and Xu, Y. (2007). A Novel Power Control Strategy of Series Hybrid Electric Vehicle. *2007 IEEE/RSJ International Conference on Intelligent Robots and Systems*, pp. 96-102.

Weisstein, E. (2021). *Energy density*. Retrieved from world of physics.

scienceworld.wolfram.com:

<https://scienceworld.wolfram.com/physics/EnergyDensity.html>.

YASA. (2021). *YASA P400*. Retrieved from Compact electric VEHICLE Motor: YASA

Ltd. YASA Limited.: <https://www.yasa.com/products/yasa-p400/>.